PBPK Model To Predict Marbofloxacin Distribution in Edible Tissues and Intestinal Exposure in Pigs

Alexis Viel, Anis Nouichi, Mélanie Le van Suu, Jean-Guy Rolland, Pascal Sanders, Michel Laurentie, Jacqueline Manceau, Jérôme Henri

A PBPK model to predict marbofloxacin distribution in edible tissues and intestinal exposure in pigs

Alexis Viel, Anis Nouichi, Mélanie Le Van Suu, Jean-Guy Rolland, Pascal Sanders, Michel Laurentie, Jacqueline Manceau, and Jerome Henri*

French Agency for Food, Environmental and Occupational Health & Safety (ANSES), Fougères Laboratory, 10B rue Claude Bourgelat, 35306 Fougères, France.

* Corresponding author at: French Agency for Food, Environmental and Occupational Health & Safety (ANSES), Fougères Laboratory, 10B rue Claude Bourgelat, 35306 Fougères, France.

Phone number: +33 (0)2 99 17 27 57 - E-mail address: jerome.henri@anses.fr

Abstract

Marbofloxacin (MAR) is a fluoroquinolone antibiotic used in food-producing animals in European Union, especially in pigs. In this study MAR concentrations in plasma, comestible tissues and intestinal segments were determined in pigs injected with MAR. Based on these data and the literature, a flow-limited PBPK model was developed to predict the tissue distribution of MAR and estimate the withdrawal period after label-use in Europe. A sub-model describing the different segments of intestinal lumen was also developed to assess the intestinal exposure of MAR for the commensal bacteria. During model calibration, only four parameters were estimated. Then, Monte Carlo simulations were performed to generate a virtual population of pigs. The simulation results were compared to the observations from an independent data set during the validation step. A global sensitivity analysis was also carried-out to identify the most influential parameters. Overall, the PBPK model was able to adequately predict the MAR kinetics in plasma and edible tissues, as well as in small intestines. However, the simulated concentrations in the large intestine were mostly underestimated, highlighting the need for improvements in the field of PBPK modeling to assess the intestinal exposure of antimicrobials in food animals.

Keywords: Marbofloxacin, pigs, food safety, residues, antibiotic resistance, PBPK

1. Introduction

In the field of food safety, antibiotic treatment of livestock poses two important public health risks: residual concentrations above the toxicity threshold in tissues intended for human consumption (the maximum residue limit, MRL), in addition to the potential selection of resistant bacteria hosted by animals when the intestinal content is exposed to the antibiotic (which could then end up in the food chain or in the environment)[1]. During assessment of these risks, it is necessary to describe, and if possible, predict the antibiotic concentrations of treated animals in order to be able to determine the exposure of tissues intended for human consumption and of the intestinal bacteria. Pharmacokinetic models based on a mathematical description with differential equations[2] are a useful tool for this purpose. The complexity of these models depends on both the purpose of the study and the available data (quality and quantity of observations). The most frequent models are called "classical" compartmental models (mono or multi-compartmental with few compartments) that reduce the organism in an empirical way but often sufficient to solve problems related to drug dosage [2]. However, these models, mostly defined by plasma data, cannot provide sufficient information for complex explorations (tissue kinetics, intestinal kinetics...) or mechanistic studies.

To overcome this, Physiologically Based Pharmacokinetic (PBPK) models are advocated for few decades[3]. These PBPK models have a structure based on the anatomical distribution of biological fluids and tissues in the body and use organism-specific parameters such as tissue volumes and local blood flow rates as well as substance-specific parameters (but with interspecies differences) such as tissue-blood partition coefficients, metabolic clearance and plasma protein binding[4]. However, the possibilities offered by PBPK modeling may suffer from a non-negligible cost due to the large number of parameters needed and their diversity, as illustrated in the modeling work presented here.

This work focused on Marbofloxacin (MAR) which is a synthetic third-generation fluoroquinolone antibiotic, marketed for veterinary use only. It acts by inhibiting the bacterial DNA-gyrase and has high antimicrobial activity *in vitro* against a wide range of gram-negative and some gram-positive bacteria and mycoplasma. It is proposed for oral or parenteral administration to cattle for treatment

of bovine respiratory disease and parenteral administration to pigs for the treatment of respiratory infections and Mastitis Metritis Agalactiae syndrome in the European Union (EU)[5], but this drug is not allowed in the US. Because of its potential for allergic reactions in humans[6] and its potential effect on the human intestinal microflora[7], residues of MAR in edible tissues (muscle, liver, kidney, skin, and fat), as for other antibiotic drugs used in farm animals, are of particular concern. The EU has established Maximum Residue Limits (MRLs) for this antibiotic in those tissues in pigs: the MRL is set at 150 µg/kg for muscle, liver, kidney and for fat (including skin), it must not exceed 50 µg/kg[6]. To manage this risk within the framework of the marketing authorization, a withdrawal period between the last MAR administration and the slaughter has been calculated and the value varies according to the commercial specialties and the European country: from 2 to 9 days[8-9].

The pharmacokinetics of MAR in pigs has already been described after intravenous, oral and intramuscular administration [10-12]. A very high intramuscular bioavailability has been observed (F_{IM} close to 100%). Similar to other fluoroquinolones, the binding of MAR to plasma proteins is low (<10%) in pigs [10]. Thus, the diffusion (unbound fraction) towards biological tissues is important [13]. MAR is mainly eliminated as an active form and largely excreted in the urine [12], with a renal clearance accounted for about half of the body clearance. The total body clearance of MAR in pigs varies greatly according to several sources [10-12, 14] ranging from 0.065 to 0.196 l/h*kg with half-lives (also depending on volume of distribution) between 4 and 14 hours.

Despite the use of parenteral routes for administration in pigs, MAR is also largely excreted into the intestinal tract. This is the case for fluoroquinolones in general and in numerous species. Despite their high bioavailability, fluoroquinolones have the characteristic of being found in significant quantities in the digestive compartment following parenteral administration. For example, 11% of the administered dose of ciprofloxacin is found in the digestive contents of humans[15], 6-7% in rats[16] and 19% in rabbits[17]. Similarly, 10% of the administered dose of enrofloxacin[18] and up to 30% for MAR[19] is found in pig faeces. Since biliary elimination of fluoroquinolones represents only 1 to 3% of the administered dose[15], the quantities found in the digestive contents following parenteral administration are therefore essentially due to intestinal elimination. Indeed, the ratios of area under

the curve (AUC) in the digestive tract and in plasma MAR ($AUC_{digestive}/AUC_{plasma}$) over 24 h were on average equals to 2 in the duodenum and to 8 in the ileum, after an intramuscular administration of 8 mg/kg in pigs[20]. During an intramuscular treatment of 2 mg/kg for 3 consecutive days, MAR concentrations between 1 and 10 mg/kg were measured in pig feces[21]. Because of the broad spectrum of activity of MAR, this molecule has the advantage of eliminating a large number of pathogenic bacteria responsible for infections. However, it also acts on bacteria from the commensal flora of the intestine [22], that could become a reservoir of resistance genes which may be then transmitted to the human flora (commensal or pathogenic) by direct contact or through the food chain [23-24].

Therefore, the objective of this study was to develop a PBPK model able to: (i) predict the residual concentrations of MAR in pigs tissues intended for human consumption in order to be able to compare them to the withdrawal period established by the EU; (ii) and adding a major innovation with the description of the observed kinetics of MAR along the digestive tract (to help predicting the selective pressure of MAR on the commensal bacteria in a future perspective). Thus, this model can be used as a mean of integrating knowledge of the pharmacokinetics of marbofloxacin in pigs but also as a tool to test the impact of alternative dosing regimens on withdrawal period or intestinal exposures.

2. Materials and Methods:

2.1 Chemicals

Marbocyl ® injectable solution (2%) was purchased from Vetoquinol, (Lure; France) for the animal experiments. MAR standard (purity > 98%) was purchased from Sigma-Aldrich (Saint-Quentin Fallavier, France). Acetonitrile and methanol were Optima ®LC/MS grade (Fisher Scientific, Loughborough, UK). The analytical grade reagents involving formic acid and isooctane were supplied by Merck (Darmstadt, Germany) and trichloracetic acid (TCA) by Fisher Scientific (Loughborough, UK). Deionized water was produced from a Milli-Q® Academic system (Millipore,

Saint Quentin en Yvelines, France). Water for injection was purchased from Lavoisier (Paris, France).

2.2 Animal experiments:

All animal procedures were carried out in strict accordance with the European directive 2010/63/EU. The protocol was approved by Ethical Committee of the French Agency for food environmental and occupational health and safety (under number 04168.01) and performed in our approved laboratory animal breeding house (Permit Number: D35-137 26).

Thirty-six crossbred female swine (Duroc x Landrace x Large White) were obtained from INRAE (Le Rheu, France). They were between 8 and 9 weeks old at reception with an average body weight of 31 kg (range from 30 to 32 kg) at the beginning of the experiments. The animals were housed in collective pens during one-week acclimation period, and then separated for the treatments. An overview of the experimental studies and their modeling purpose is presented in table 1.

2.2.1 Surgery

For pigs receiving MAR by intravenous route, central venous catheters were implanted. These animals were firstly sedated with an IM injection of ketamine at 20 mg/kg (Imalgène, Mérial, Lyon, France) and xylazine at 2 mg/kg (Rompun, Bayer, Loos, France). Then, they were intubated and kept anesthetized by inhalation with isoflurane 2.5% (IsoFlo, Zoetis, Malakoff, France) during all the surgical procedure. An incision was performed on the neck under local anaesthesia with xylocaine (Xylovet, CEVA, Libourne, France). After dilaceration of superficial tissues and muscles, two catheters were implanted in the jugular vein, one for drug administration and one for blood sampling. Catheters were maintained by polyglactine suture (Vetsuture, Paris, France). After surgery, pigs were allowed to recover in their box for at least three days before the study was initiated. Then, they were housed separately in metabolism cage in order to facilitate drug administration and blood sampling.

2.2.2 Experimental setup for partition coefficients determination and model calibration

For the model calibration, two datasets were used. The first one (called “Study A”) is an in-house study where eighteen catheterized pigs received a 4h-constant intravenous (IV) infusion of MAR (Marbocyl®) at 4 mg/kg BW/24h, preceded by a loading dose of 1 mg/kg BW. These 18 pigs were randomized into six batches of three individuals each.

Five of these batches were used for a depletion study where each batch of pigs was respectively sacrificed at 4, 8, 15, 18 and 24 h after the loading dose (i.e. 0, 4, 11, 14 and 20 h after the end of infusion). This depletion study corresponded to a PK destructive sampling (i.e. only one time point per animal). The sixth batch of three pigs was sacrificed 4h after the loading dose (i.e. when steady state was reached) to get the partition coefficient values (see 2.4.1).

All tissue samples (muscle, liver, kidney, abdominal fat, and skin) and the different gut lumen segment contents after scrapping (duodenum, proximal jejunum, distal jejunum, ileum, proximal colon and distal colon) were taken; blood was also taken and kept in heparinized tubes, centrifuged (3000 g for 10 min) and the plasma was collected. All samples were quickly stored at -20°C before MAR quantification by High Performance Liquid Chromatography (HPLC) (see section 2.3).

The concentrations associated to the samples of these five first batch were used to develop and calibrate the PBPK model (see 2.4). Those of the sixth batch were used to determine the tissue: plasma partition (P_x) coefficients of MAR in the different pig edible tissues. P_x were calculated as follows:

$$\mathrm{Px} = \mathrm{Cx\_ss} \,/\, \mathrm{Cplas\_ss} \qquad \text{Eq. (1)}$$

where P_x is the partition coefficient of the tissue x, C_{x_ss} is the MAR concentration measured at steady-state in the overall tissue x, i.e. containing both extracellular and intracellular spaces; C_{plas_ss} is the plasma concentration of MAR at steady-state.

The second dataset (with all the raw data) used for the calibration step (called “study B”) was kindly provided by Ferran et al., based on a published study [20]. Briefly, twenty-four (24) male pigs aged 2–

4 months and weighing 14–28 kg were used to assess plasma, bile and intestinal content MAR concentrations in parallel over 24 h. Pigs received a single intramuscular (IM) administration of 8 mg/kg MAR in the neck. Three pigs were randomly sacrificed at 1.5, 2, 4, 6, 9, 12 and 24 h after MAR administration. Immediately after sacrifice, the contents of the gall bladder (data provided by the authors), small intestine segments (duodenum, proximal jejunum, distal jejunum, and ileum) and large intestine (proximal and distal colon) (data provided by the authors), of each pig were sampled. Plasma samples were taken 1h after MAR administration and at slaughter time for each pig (i.e. 2 samples per pig).

2.2.3 Experimental setup for PBPK model predictive ability (validation)

In order to check model predictive ability a validation in-house study (called "study C") was conducted. Eighteen pigs received a single daily injection by IM route (neck) of 2 mg/kg BW of MAR (Marbocyl®), during three consecutive days (corresponding to the recommended dosing regimen). Three pigs were sacrificed at each sampling times i.e. at 54, 72, 78, 96, 102 and 168h after the first administration. Samples of thigh muscle, injection site (100 g of the whole tissue around the sting mark), liver, kidney, abdominal fat ,skin, and intestinal segments content were immediately collected and taken over, in the same way as in the preceding experimental setup (see 2.1.1), before MAR quantification with the same analytical methods.

Table 1. *Experimental studies of Marbofloxacin in pigs used for calibration and validation of the PBPK Model.*

Modelling purpose	Study ID	Route and doses	BW (kg)	n	Matrix
Model calibration and partition coefficients determination	A*	loading IV dose of 1 mg/kg BW then 4h constant IV infusion at 4 mg/kg BW/24h	31	18	P, M, L, K, S, F, D, PJ, DJ, I, PC, DC
Model Calibration	B[20]	single IM administration of 8 mg/kg BW	14–28	24	P, B, D, PJ, DJ, I, PC, DC
Model Validation	C*	Triple IM administration of 2 mg/kg BW	31	18	P, M, IS, L, K, S, F, D, PJ, DJ, I, PC, DC
	D[13]	single IM administration of 2.5 mg/kg BW	21-23	40	P, M, IS, L, K

IV: intravenous, IM: intramuscular, P: plasma, M: muscle, L: liver, K: kidney, F: abdominal fat, S: skin, D: duodenum, PJ: proximal jejunum, DJ: distal jejunum, I: ileum, PC: proximal colon, DC: distal colon, B: bile, IS: injection site. Sources: *Current study; [20](Ferran *et al*., 2013); [13](Yang *et al*., 2017).

2.3 Analytical method

2.3.1 Sample preparation

Extraction and purification of samples were realized by adaptation of a previously published method [1]. Briefly, 200 µl of plasma were mixed with 0.8 ml of 5% TCA, and then centrifuged. For tissues, 2 g of sample were mixed with 8 ml of 5% TCA, and then centrifuged. For fat and skin samples, 2 ml of isooctane were used to improve the extraction of these rich in lipids matrices. After centrifugation (20000g, 5 min) the supernatant was filtered through a 0.45µm syringe filter and 100 µl were injected in HPLC system.

2.3.2 HPLC analysis

MAR was determined by high-performance liquid chromatography equipped with a fluorescence detector (Agilent 1100 Series HPLC System, Agilent Technologies, Les Ulis, France). Emission wavelength was set at 299 nm and excitation at 505 nm. The mobile phase consisted of a linear gradient of 0.1% formic acid (A) and acetonitrile (B) as follows: 0-5min 3-30% B, 5-5.7 min 30% B, 5.7-5.8 min 30-3% B. Separations were carried out using a Nucleodur C18 Gravity column (125 mm x 4 mm, 5µm) (Macherey-nagel, Hoerdt, France) at 25°C with a flow rate of 0.8 ml/min. The analytical method performances (trueness, precision) were assessed using an approach based on total error (accuracy profile). The e-noval software (version 3, Arlenda, Liège, Belgium) was used to perform this assessment. Analytical methods performances are detailed in table2, with lower limits of quantification (LLOQs) of 25.0 µg/L for plasma, 20.3 µg/kg for kidney and 15.1 µg/kg for the other tissues (i.e., muscle, liver, fat and skin).

For each matrix to be analyzed, performances of the analytical methods (including limits of quantification, LOQ or detection LOD) were established (Supplementary materials, Table S2) during

their validation. The LOD is the limit below which the analyte is considered as not detected, with a certain associated probability. It is estimated according to Equation 2:

$$\mathrm{LOD} = 3.3 * \frac{\mathrm{Sao}}{\mathrm{a1}} \qquad \text{Eq. (2)}$$

With Sao the standard deviation of the intercepts of the calibration lines and a1 the slope of the calibration line (sensitivity). As for LOQ, it generally represents the lowest concentration in a sample that can be quantified with acceptable accuracy under specified experimental conditions.

2.4 PBPK Modeling

2.4.1 Model structure and parametrization

The tissue part of the PBPK model was described by a flow-limited approach with well-mixed compartments corresponding to liver, kidneys, muscles, fat, skin, gut wall, gallbladder and the plasma (venous and arterial together) where the IV dose is administered. The IM injection site was also described for IM administration. The remaining part of the body (without the digestive tract, see below) was lumped[25] into a compartment named “Rest” (see figure 1 for the diagram of the model). Each tissue compartment was defined by (i) a tissue volume and blood flow (species-specific physiological parameters), except the intestinal lumen and gallbladder compartments defined only by a volume; (ii) a partition coefficient Px (chemical-specific parameter), representative of the affinity of the molecule for the organ defined each tissue compartment. The Px were calculated as described in 2.2.2 except for the lumping compartment (Prest) which was calculated as described elsewhere[18]: it was defined as the weighted mean of the partition coefficients of the lumped organs, separated between poorly and richly perfused tissues (Equation 3). A threshold of <100 ml/min/100 g tissue weight was used to define the poorly perfused tissues[26]. The partition coefficient of the kidneys (Pkidneys) was used for richly perfused tissues (heart, pancreas, spleen, lungs) and the partition coefficient of the muscle (Pmuscle) was used for poorly perfused tissues (carcass and brain).

$$Prest = \frac{\text{Pmuscle} \times \text{Vpoorly}_{\text{perfused}} + \text{Pkidney} \times \text{Vrichly}_{\text{perfused}}}{\text{Vpoorly}_{\text{perfused}} + \text{Vrichly}_{\text{perfused}}} \quad \text{Eq. (3)}$$

Where $Vrichly_{perfused}$=$FracVHeart + FracVPancreas + FracVSpleen + FracVlung$

and $Vpoorly_{perfused}$= $FracVCarcass + FracVbrain$

Thus, drug distribution in each non-eliminating tissue compartment (except IM injection site, intestinal lumen and gallbladder compartments) was described by the following ordinary differential equation:

$$\frac{\text{dCx}}{\text{dt}} = \frac{\text{Qcx}}{\text{Vx}} \times (\text{Cplasma} - \frac{\text{Cx}}{\text{Px}}) \quad \text{Eq. (4)}$$

Where Qc_x is the plasma flow within the tissue x, V_x is the tissue volume, P_x the partition coefficient, C_{plasma} the plasma concentration and C_x the concentration in the tissue x.

Due to a different configuration of vascularization, the liver, and the gut wall are exceptions to this equation (see Table S5 for the model code). Briefly, the portal veins were unified into a single blood flow ($Qc_{Gutwall}$ in Fig. 1) that represents a passageway for MAR's transport into liver. Moreover, hepatic plasma output flow was modeled as the combination of hepatic arterial and portal veins (flows combined in the structural parameter Qc_{Liver} in Fig 1.) as described in another published PBPK model of MAR in poultry[27].

Regarding the intestinal lumen sub-model, the different segments (duodenum, proximal jejunum, distal jejunum, ileum, proximal colon, and distal colon) were modeled differently (Fig 1.): unidirectional flows of intestinal contents and thus, MAR quantities along the lumen, were described with first-order transit constants linking these compartments.

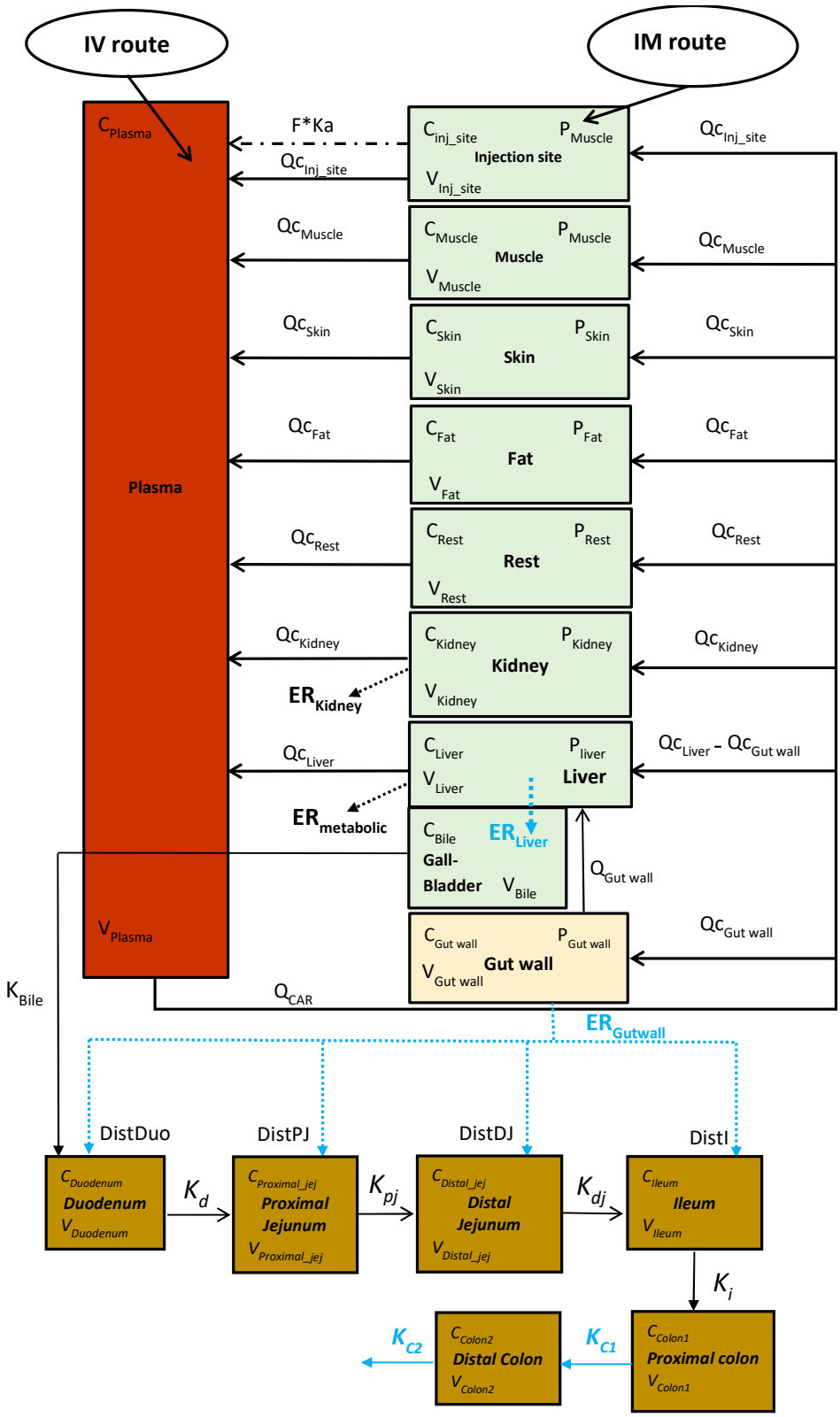

Figure 1. Diagram of the PBPK model (see Table 2 for abbreviations). Parameters in blue were estimated during calibration. C_X represent the concentrations in each compartment, V_X represent the volume of each compartment, P_X represent the partition coefficient of each vascularised compartment, Qc_X represent the

261 blood flow to each vascularized compartment, ER_X represent the extraction ratios of each route of elimination
262 and K_X represent the constants of transit within the intestines.

263 The values for physiological structural parameters of the different tissue compartments in pig were
264 collected from various published articles as detailed in Table 2. In this table, volumes are expressed
265 as percentage of bodyweight before being multiplied by the observed individual bodyweight of pigs.
266 The density of plasma and tissues were assumed to be 1 kg/L. For pigs, an haematocrit (H) value of
267 41.2% [28] and a cardiac output (Qcar) value of 8.7 L/h/kg BW [28] were used. The cardiac output was
268 first transformed into a plasma total output (QTOT) with the formula:

$$\mathrm{QTOT} = (\mathrm{Qcar\ x\ Bodyweight})\ \mathrm{x}\ (1 - \mathrm{H}) \qquad \text{Eq. (5)}$$

269 Then, QTOT was multiplied by the fractions of regional blood flow in each tissue compartment
270 $FracQc_x$ (detailed in table 2) to get the flow within each tissue (Qc_x). Unlike other compartments, the
271 plasma volume was converted from the blood volume ($FracV_{BLOOD}$) according to the haematocrit with
272 this formula[27]:

$$V_{PLASMA} = (FracV_{BLOOD}\ x\ Bodyweight)\ x\ (1 - H) \qquad \text{Eq. (6)}$$

273 The value of bile volume was taken from published article [29] and set as a constant value without
274 taking pulsatile secretion into account.
275
276 Finally, the total body clearance value found in Ferran et al.[20] was selected and fixed during the
277 calibration. This value was split between the different clearance routes. Indeed, a previous study in
278 pigs found that the elimination due to the renal clearance ($FracE_{kidney}$) accounts for about 52% of the
279 administered dose (eliminated in urine as unchanged drug), and that about 6.5% of the parent
280 compound is eliminated by hepatic biotransfomation ($FracE_{metabolic}$)[12]. Due to the fact that
281 fluoroquinolones are substrates of some efflux transporters such as the ATP-Binding Cassette (ABC)
282 superfamily[30], we added the intestinal ($FracE_{gutwall}$ parameter) and biliary secretions ($FracE_{bile}$
283 parameter) as additional routes for the clearance of MAR. Their respective excretion fractions were

284 estimated during the calibration, ensuring that the sum of all excretion fractions (renal, metabolic,
285 biliary and intestinal) was equal to one. The resulting fraction of intestinal secretion was then sub-
286 divided (according to DistDuo, DistJP, DistJD and DistI parameters) among the different segments
287 of the small intestine, based on the expression of P-gp protein measured in pigs [31-33]. The bile flow
288 (WK_{bile}) from gallbladder to duodenum was also extracted from the literature[34].
289 Concerning intestinal transit, parameters were calculated based on experiments and literature. From
290 the different lengths of the intestinal compartments obtained experimentally (during Study A), we
291 deduced the volumes of the intestinal contents as well as the transit constants based on (i) the
292 calculation of Merchant et al. for the volume correspondences of contents per cm of intestine[35]; (ii)
293 the data from Wilfart et al. which described the average retention time in hours in the small intestine
294 and colon for low-fiber food bowls[36], that were divided according to the measured lengths.
295
296 As IM injection is the labelled route of administrations for MAR in pig, the IM bioavailability (F) and
297 the IM absorption constant (k_a) were used for the intramuscular experiments and the IM doses
298 (individually embedded in the dataset) were incorporated in the injection site compartment. The
299 corresponding volume fraction for the injection site ($FracV_{InjSite}$) was fixed to 0.3% of bodyweight (100
300 g). Fraction of cardiac output to injection site ($FracQc_{InjSite}$) was set to 0.9% and the partition
301 coefficient of the injection site ($P_{Injsite}$) was assumed to be identical to that of the muscle (P_{Muscle}), as
302 already parametrized elsewhere [37]. Thus, no need to calibrate any parameter of this compartment
303 before the predictive ability check.

304 All structural parameters are detailed in Table 2. As often as possible, values were obtained from
305 published sources or experimentally determined in order to estimate as few structural parameters
306 as possible, for a better plausibility of the model.

307 ***Table 2**. Structural parameters (fixed effect) of the PBPK model.*

Abbreviations	Descriptions	Units	Values	Sources
Species-specific physiological parameters				
Q_{CAR}	Cardiac output per kg of bodyweight	L/h/kg	8.7	[28]
H	Haematocrit	%	41.2	[28]
$FracQc_{InjSite}$	Flow fraction to IM injection site	%	0.9	[37]
$FracQc_{Muscle}$	Flow fraction to muscles	%	29.2	[38]
$FracQc_{Fat}$	Flow fraction to fat	%	11	[38]
$FracQc_{Skin}$	Flow fraction to skin	%	3.5	[28]
$FracQc_{Kidney}$	Flow fraction to kidney	%	9.8	[38]
$FracQc_{Liver}$	Flow fraction to liver	%	22.5	[38]
$FracQc_{GutWall}$	Flow fraction to gut wall	%	18	[39]
$FracQc_{Rest}$	Flow fraction to the rest of the body	%	23.1	100 minus sum of the other fractions
$FracV_{InjSite}$	Volume fraction of IM injection site	%	0.3	[37]
$FracV_{Muscle}$	Volume fraction of muscles	%	45	[38]
$FracV_{Skin}$	Volume fraction of skin	%	5.28	[28]
$FracV_{Fat}$	Volume fraction of fat	%	17.6	[38]
$FraV_{Liver}$	Volume fraction of liver	%	1.7	[38]
$FracV_{Kidney}$	Volume fraction of kidneys	%	0.3	[38]
$FracV_{GutWall}$	Volume fraction of gut wall	%	5.19	Experimental
$FracV_{Blood}$	Volume fraction of blood	%	4.12	[28]
$FracV_{Rest}$	Volume fraction of remaining body	%	15.4	100 minus sum of the other fractions
$FracV_{DUODENUM}$	Volume fraction of duodenum	%	0.18	Experimental
$FracV_{JEJUNUM1}$	Volume fraction of proximal jejunum	%	1.8	Experimental
$FracV_{JEJUNUM2}$	Volume fraction of distal jejunum	%	1.8	Experimental
$FracV_{ILEUM}$	Volume fraction of ileum	%	0.18	Experimental
$FracV_{COLON1}$	Volume fraction of proximal colon	%	0.46	Experimental
$FracV_{COLON2}$	Volume fraction of distal colon	%	0.77	Experimental
$FracV_{bile}$	Volume of bile	%	0.175	[29]
WK_{bile}	Bile excretion flow	L/h/kg	0.002	[34]
Chemical-specific parameters				
ka	IM absorption constant	h^{-1}	5.85	[40]
F	IM bioavailability	%	100	[12]
P_{Muscle}	Partition coefficient of muscles	No unit	1.66	Experimental
P_{Fat}	Partition coefficient of fat	No unit	0.33	Experimental
P_{Skin}	Partition coefficient of skin	No unit	0.63	Experimental
P_{Liver}	Partition coefficient of liver	No unit	1.73	Experimental

P_{Kidney}	Partition coefficient of kidneys	No unit	3.44	Experimental
$P_{GutWall}$	Partition coefficient of gut wall	No unit	0.83	[4]
P_{Rest}	Partition coefficient of the rest of the body	No unit	1.98	Calculated[25]
WCLTOT	Total clearance	L/h/kg	0.16	[20]
For P_{rest} calculation				
$FracV_{Carcass}$	Volume fraction of the carcass	%	9.3	[38]
$FracV_{Heart}$	Volume fraction of heart	%	0.4	[38]
$FracV_{Pancreas}$	Volume fraction of pancreas	%	0.169	[41]
$FracV_{Spleen}$	Volume fraction of spleen	%	0.74	[42]
$FracV_{Brain}$	Volume fraction of brain	%	0.1	[38]
$FracV_{Lung}$	Volume fraction of lung	%	0.8	[38]
Intestinal transit				
Kd	Duodenum transit constant	h^{-1}	5.26	Calculated based on experiments and literature [35-36]
Kjp	Proximal jejunum transit constant	h^{-1}	0.51	Calculated based on experiments and literature [35-36]
Kjd	Distal jejunum transit constant	h^{-1}	0.51	Calculated based on experiments and literature [35-36]
Ki	Ileum transit constant	h^{-1}	5.26	Calculated based on experiments and literature [35-36]
Kc1	Proximal colon transit constant	h^{-1}	0.48 (study A) 5.16 (study B)	Estimated for each study separately
Kc2	Distal colon transit constant	h^{-1}	1.03 (study A) 6.64 (study B)	Estimated for each study separately
Distribution of the elimination routes				
FE_{KIDNEY}	Fraction of excretion in the kidneys	%	52	[12]
$FE_{METABOLIC}$	Fraction of elimination as metabolites	%	6.5	[12]
$FE_{GUTWALL}$	Fraction of excretion in the gut wall	%	41	Estimated
FE_{BILE}	Fraction of excretion in the Bile	%	0.49	Estimated
$FE_{GUTWALL}$ Sub-division Values (based on P-gP expression):				
DistDuo	Distribution value in duodenum	%	15	[31-33]
DistPJ	Distribution value in proximal jejunum	%	25	[31-33]
DistDJ	Distribution value in distal jejunum	%	30	[31-33]
DistI	Distribution value in ileum	%	30	[31-33]

2.4.2 Model Calibration

Regarding the structural model, only 4 parameters had to be estimated (see table 2): $FE_{GUTWALL}$ and FE_{BILE}, for which the value was unknown, as well as the transit constants within colon (Kc1 and Kc2) for which the range of values was very large and variable in the literature. Indeed, for the latter the range for the transit time was 26–44 h in the study of Wilfart et al.[36] and 55-169h in the study of Henze et al.[43].

No inter-individual variability (IIV) was considered during this calibration step due to the experimental design based on destructive sampling used in study A and B, therefore only typical values were estimated. However, different values between Study A and Study B were estimated for Kc1 and Kc2 due to the high variability in the observed data and the high associated uncertainty (as explained above). For the error model, there were as many residual variabilities (RVs) as there were observations compartments; and the RVs were also assumed to be different between study A and B, due to different analytical method, design and experimental conditions. To avoid negative results, the dataset was log-transformed and the error model was assumed to be constant (i.e. equivalent to a proportional error model with non-transformed data). The estimation of all these parameters was carried out using the SAEM algorithm [44] implemented in Monolix©. Data below the LOQ were treated as left-censored (i.e., the likelihood that they were between zero and the LOQ was calculated) [45]. The relative standard errors (RSE) were calculated to assess precision of estimation. Model building was based on the plausibility of the physiology, the values of RSE (<30%) and the Visual Predictive Checks (VPCs) with a 90% prediction interval.

2.4.3 Establishment of the population PBPK (popPBPK) model and validation (model predictive ability)

After calibration, Monte Carlo simulations were performed to generate a virtual population of (n = 1000) pigs. A log-normal distribution was assumed for the inter-individual variability (IIV) of all parameters because of their asymmetric distribution and their strictly positive values[46-47]. Nevertheless, there were exceptions for $FE_{GUTWALL}$, FE_{BILE}, FE_{KIDNEY} and $FE_{METABOLIC}$ for which a logit-

normal distribution was assumed because of their values which should be between [0-1] range. Coefficients of variation (CV) were set at 30% for physiological and 20% for drug-related parameters. The code (see Table S5) was written so that the sum of the volume fractions, the blood flow fractions and the fractions of the total clearance for elimination (either by excretions or metabolism) did not exceed 1, respectively [47-48].

This virtual population received three intramuscular (IM) administration of MAR at 2 mg/kg BW, based on the dosing regimen used in study C (see Table 1), and the 98% prediction distributions of the predicted concentrations were plotted against this in-house validation dataset (study C, independent of those used for calibration) as a model diagnostic. If predictions fell within a 2-fold of the experimental data, the model was considered to be reasonable and acceptable according to World Health Organization (WHO)[49] and Organization for Economic Co-operation and Development (OECD)[50] guidelines; the 3-fold errors was also used similarly to previous studies [51-52]. The goodness-of-fit was further evaluated with (i) a linear regression analysis with calculation of the determination coefficient (R^2) and (ii) the mean absolute percentage error (MAPE) calculation between model predictions and average measured MAR concentrations in tissues (plasma, skin, muscle, abdominal fat, liver & kidney) and in gut lumen (duodenum, proximal and distal jejunum, ileum, proximal and distal colon). The popPBPK model was considered as valid if R^2 was at least 0.75 and the MAPE was lower than 50%[47, 53]. As a supplementary verification of the predictive ability of the model, another simulation was carried-out to be compared with the only other available publication giving MAR tissue data in pigs (Study D)[13], using the typical plasma clearance extracted from their data (0.08 L/h/kg). The simulated dosing regimen was a single IM administration of 2.5 mg/kg of MAR.

An estimation of the withdrawal period (WP) in kidney was also performed using the popPBPK model, based on the results of the Monte Carlo simulations with the standard dosing regimen specified in the summary of product characteristics (SPC) of the Marbocyl® speciality (corresponding to the experimental design of study C). The time (rounded up to the next whole day) for which the 99th percentile is equal to the MRL (150 µg/kg) since the last injection in kidney was defined as the (predicted) WP, because the 99th percentile can give results similar to the 95%

tolerance limits used in the EU[54]. This value was compared to the official WP for Marbocyl® in the EU (3 or 4 days depending on the country), as indicated on the EMA website[9].

2.5 Global sensitivity analysis

Global sensitivity analyses (GSA) using the "extended-FAST" method[55], were performed with all parameters (52 parameters). The first output was the maximal concentration in kidney after the last administration ($C_{max(49h)}$) because kidney is the limiting organ for the determination of the withdrawal period of MAR in pig, and Cmax is one of the key factors driving this value. A second GSA was carried-out with the $AUC_{(0-75h)}$ in ileum as output because it seems relevant for the issue of pressure of selection regarding the resistance to MAR in the intestinal *E. coli* population[20].

The GSA orders the inputs by importance, identifying the main contributors to the variation in the chosen model outcomes. A uniform distribution was considered and each parameter was changed by ±10% of the median value, simultaneously [47, 56]. With the GSA, input parameter influence could be divided into main effects and total effects where the difference between main and total effects (additional effects) represented parameter interactions. Total effects above the typical threshold value of 0.1 (10%) indicated significantly sensitive parameters [57-59] and only those ones were reported.

2.6 Softwares

MonolixSuite®(2021R1) [60] was used to develop the PBPK model using the Mlxtran language [61]. Simulx© [62] was used to run all simulations. RStudio [63] was used to plot the simulations against the in-house validation dataset and to perform the GSA using the sensitivity package[64] and lixoftConnectors package[65] . The graphs resulting from the GSA were made with MS Excel[66]. MS Excel was also used to carry out the regression analyses and the graph of predictions/observations ratios.

3. Results

3.1 Model calibration

During the calibration process, there were 16 BLQ (below the limit of quantification) data (8.9% of all data) which were treated as left-censored data (7 duodenum samples,7 proximal jejunum samples, 1 distal jejunum sample and 1 ileum sample) from study A (Table S3). Moreover, for 5 skin samples, 3 ileum samples and 2 distal colon samples, MAR could not even be detected (< LOD).

The model included fifty-two structural parameters of which only four were estimated: $FE_{GUTWALL}$, FE_{BILE} and the colon transit constants (Kc1 and Kc2, different for each study). These 4 structural parameters were well estimated as well as the RVs (see Table S1), with a good confidence (RSE <30%). The transit rates in colon (Kc1 and Kc2) were estimated at very different values between both studies, with the fastest transit being for Study B (6 to 10 times higher values). The RVs were on average higher in the intestinal segments (up to 150%) compared to the edible tissues and plasma, highlighting the huge observed variability of these data. Overall, the VPCs in plasma, tissues and intestinal segments (see Figures S1, S2, S3 and S4) displayed a good agreement between observed data and predictions for both studies (A and B), except an underestimation of observed data at late times for plasma in study B (Fig. S2), kidney (Fig. S1), small intestines and large intestine (for study B only, Fig. S3-S4).

3.2 Population PBPK model simulations and validation (model predictive ability)

One thousand virtual pigs receiving three IM administration (2 mg/kg BW) were generated thanks to Monte Carlo simulations and the 98% prediction intervals were plotted against the in-house validation dataset (study C), to check the predictive ability of the model for the plasma and each edible tissue (Figure 2), as well as for the digestive tract contents (Figure 3). Overall, this validation dataset was composed of 52% quantifiable data, 26% of BLQ data (mostly in the digestive segments) and 22% of non-detectable concentrations.

For edible tissues and plasma, at the last sampling time (*i.e.* at 168h after the first administration), all tissue data except one injection site sample were below the LOD and all the plasma data were BLQ (Fig. 2). Unexplainable rebounds (not observed on the calibration dataset, see Fig. S1 and S2) were observed in the plasma data, especially at T=102h. The kidneys were the organ with the highest MAR concentrations at T=96h (average of 33.4 µg/kg for two pigs, excluding the sample < LOQ). Overall, only one observation in the injection site were outside the 98% prediction range of the model (Fig. 2). The observations below the LOQ for all tissues were also inside the 98% prediction range of the model although the true value of these observations is subject to uncertainty. Furthermore, the central tendency of the simulations respected the final elimination slopes of the observed data. The period between the last administration and the tissue concentration falling below the MRL was equal to 73h, 60h, 51h, 57h, 69h and 80h for muscle, injection site, fat, liver, skin and kidney respectively. Therefore, based on the simulations in kidneys, the predicted WP was rounded to 4 days.

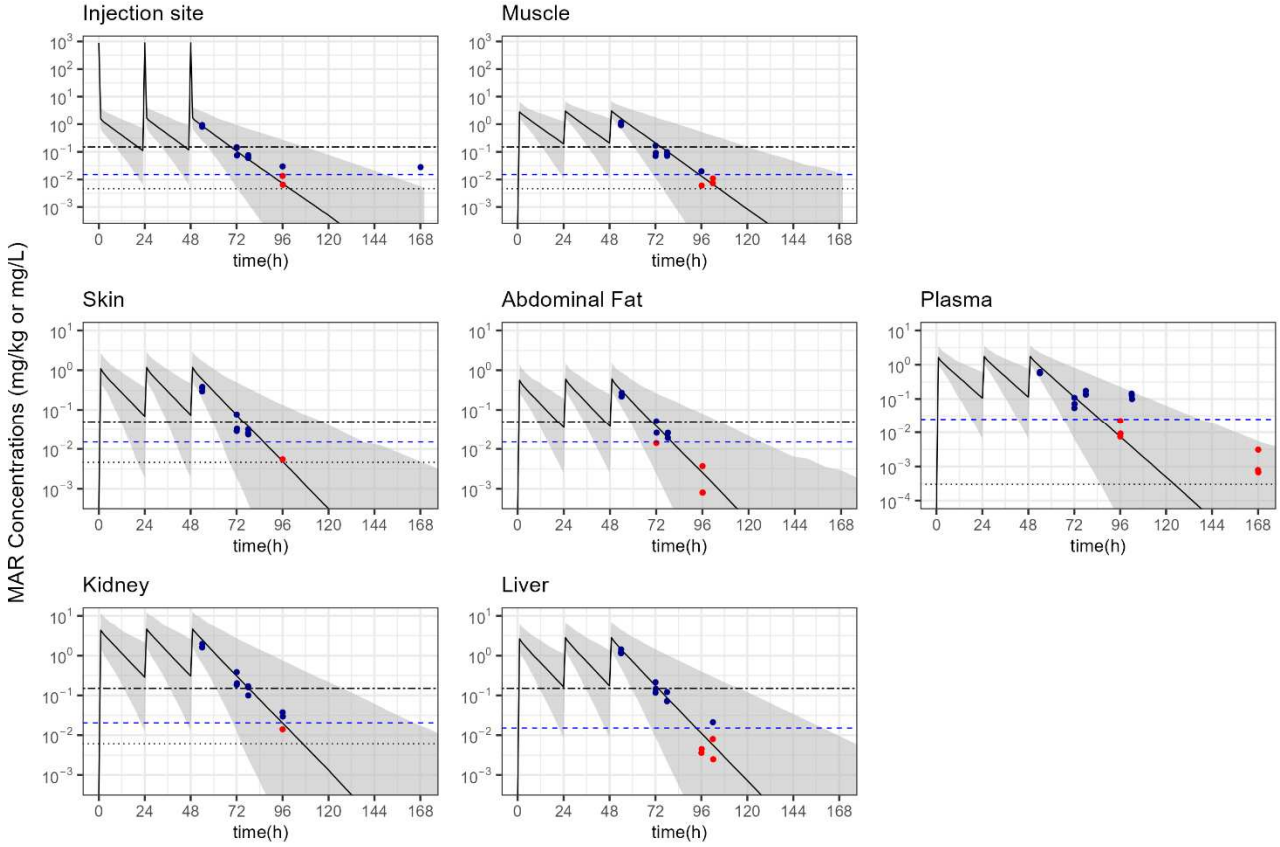

Figure 2. Distribution of predictions against observations (Study C) in tissues and plasma at the end of the triple IM treatment, in semi-log scale. The solid black lines represents the median, grey areas represent 98% prediction intervals,

blue and red points represent the observations above and below the LOQ, respectively. Dash-dotted black line represents the LMRs in edible tissues. Dashed blue line represents the LOQ and the dotted black line, the LOD. Of note, data below the LOQ were plotted at their measured value although the true value of these observations is subject to uncertainty.

Regarding the digestive segments (Figure 3), the observed concentrations quickly fell below the LOQ (at t=72-78h) except for the two parts of the colon where MAR concentrations were above the LOQ until 96h. The majority of observations in small intestines were inside the 98% prediction interval of the model with only one observations in proximal jejunum outside this interval (2% of the total observations in the small intestine). The observations below the LOQ were all inside the 98% prediction range of the model. There were nonetheless a significant underestimation by the model of the central trend for the proximal and especially distal colon, even if the terminal slope in the proximal colon was similar to that of the observed data.

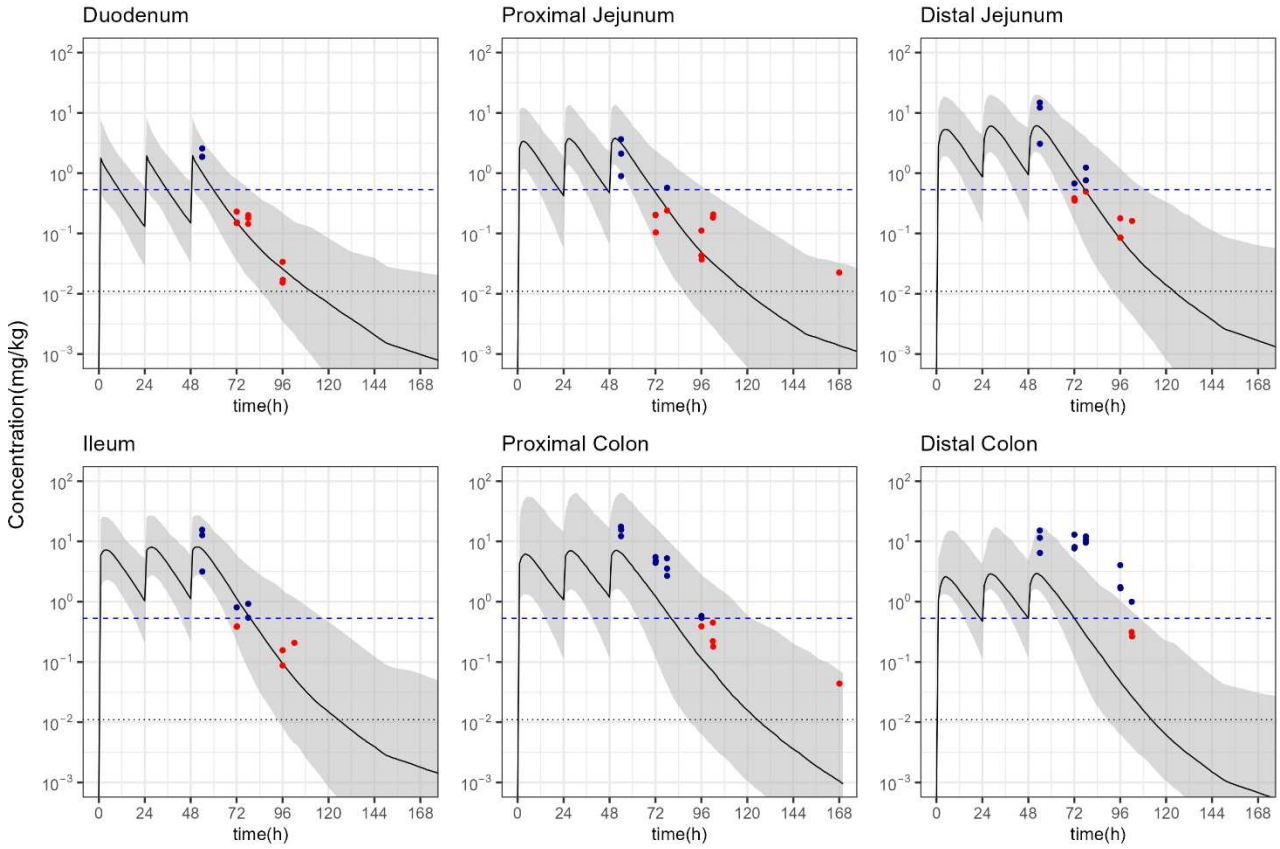

Figure 3. Distribution of predictions against observations (Study C) in the different intestinal segments at the end of the triple IM treatment, in semi-log scale. The solid black lines represent the median, grey areas represent 98% prediction interval, blue and red points represent the observations above and below the LOQ, respectively. Dashed blue line represent

the LOQ and the dotted black line, the LOD. Of note, data below the LOQ were plot at their measured value although the true value of these observations is subject to great uncertainty.

The result of the regression analysis between model median predictions and measured MAR concentrations is presented in Figure S5. The coefficient of determination (R^2) was 0.5 for all tissues. Separately, it was 0.95, 0.71 and 0.45 for edible tissues with plasma, small intestine and large intestine, respectively. MAPE values were acceptable for plasma and edible tissues (44.1%), and for the small intestines (37.9%) but too high for the colon (>50%).

The percentage of predictions within 2-fold errors (Figure S5) of the experimental data was 76.5% for all observed data including plasma, edible tissues, and gut lumen. Separately, it was very good in plasma and edible tissues with a value of 89.6% but decreased to 30% for gut lumens (68% for small intestines only). Furthermore, the percentage of predictions within 3-fold errors (Figure S5) increased to 85.6% for all observed data; separately, it was 95.8% in plasma and edible tissues, 94.8% for small intestines alone and fell to only 48.8% when considering the whole gut lumen.

We also assessed the ability of the PBPK model to predict the mean tissue and plasma MAR data from the study of Yang et al.[13] (see Fig S6). All observed data were included within the 98% prediction interval except for the muscles, kidneys and injection site concentrations at the early time points.

Overall, the popPBPK model was considered valid for plasma, edible tissues and the contents in the small intestines (duodenum to ileum).

3.3 Global sensitivity analysis

Two GSA were carried out with the fifty-two parameters of the PBPK model and the results are presented in supplementary materials (Figure S7). The variability of C_{max} in kidney at the end of treatment ($C_{max(49h)}$) and of the $AUC_{0\text{-}75h}$ in ileum was mainly due to the main effects of several structural parameters (rather than the interactions between the structural parameters). The most influencing parameters (Sensitivity coefficient > 10%) for $C_{max(49h)}$ were (in order of importance) the

bodyweight (BW), the total clearance (WCL_{TOT}), partition coefficient of muscle (P_{Muscle}) and partition coefficient of kidney with sensitivity coefficient of 88.8%, 25.7%, 21.8% and 15.5%, respectively (see Figure S7A). Regarding the second output ($AUC_{0\text{-}75h}$ in the ileum), WCLTOT and BW were also among the most influential parameters with sensitivity coefficient of 88.7% and 33.0%, respectively. As expected, the transit constant Ki (35.7%) and the volume of ileum content $FracV_{Ileum}$ (33.8%) were also significant parameters (see Figure S7B).

4. Discussion

The aim of this work was to build and validate a PBPK model for marbofloxacin in pigs (with two original datasets and two datasets coming from the literature) in order to study the tissue distribution (for assessing the risk of exceeding regulatory limits in edible tissues) and also the intestinal concentration kinetics (with the aim of exploring the risk of selecting bacterial resistance in the different gut segments). The “classic” PBPK models (in chemical risk assessment and food safety) for farm animals including edible tissues[67-68] are well known and widely used; however linking a PBPK model with a sub-model of excretion into and transit through the gut lumen segments of pigs, to describe observed data in it, is an innovation that raises some challenges, as discussed below. Overall, the evaluation of the PBPK model of MAR in pigs is summarized in Table S4 according to the WHO criteria[49].

Firstly, it should be noted that the outputs of this PBPK model are in agreement with the volume of distribution and clearance found in previous pharmacokinetic results for marbofloxacin in pigs. Indeed, the volume of distribution was calculated[69] from this PBPK model and the value of 1.24 L/kg was obtained. This value is close to that obtained experimentally[12]. As mentioned in introduction, the total body clearance of MAR in pigs varies greatly according to physiological state (age, pregnancy,…)[10-12, 14] and using the most relevant value of total clearance in the PBPK model is sufficient, according to corresponding physiological state, so that it is automatically subdivided in its various components (renal, hepatic and intestinal). However, it is possible that this subdivision scheme is modified by the physiological state itself. In this case, a more mechanistic model taking

into account the impact of changes in physiological mechanisms would be needed. But for this to happen, significant progress must be made in the bottom-up approach[70] in the farm pig.

Overall, the PBPK model correctly predicted the vast majority of available data on plasma and edible tissues (skin, abdominal fat, liver, kidney, muscle and even injection site for Study C) as well as the concentrations in the different small intestine segments as highlighted by the relatively good R^2 and MAPE values. Regarding the results for the injection site of Study D (see Fig S6), the predictions were not in good agreement at the early time points and the data were overall underestimated. However, it is known that injection sites often show erratic PK profiles that will notably depend on the volume of injection, method used to collect them and other factors[71-72].

Regarding the large intestine concentrations of MAR, they were overall underestimated during the calibration for study B (see Fig. S4) and also for study C during the validation step (figure 3) and this limitation is discussed below. Nevertheless, most of the model parameters (48 parameters) were fixed according to the literature in order to maximize the physiological plausibility. Thus, the optimization concerned only four parameters of the structural model ($FE_{GUTWALL}$, FE_{BILE}, Kc1 and Kc2), as well as the RVs of the calibrated compartments (n=13). This optimization did not pose any identifiability or estimation problems (low RSEs).

Partition coefficients (Px) were experimentally determined at equilibrium in each edible tissue (Table 2), and thus the model was able to correctly predict MAR concentrations in these tissues of interest (kidney, muscle, liver, skin and abdominal fat) (Fig. 3). The kidney was the organ with the highest affinity for MAR highlighted by its Px (Pkidney = 3.44) being about 2 to 10 times higher than for the other tissues. This is similar to published Px values in poultry, also experimentally determined, that were used to develop a PBPK model in this species[27] but higher than a previous study in pigs[13]. In this study, the partition coefficients were generated at steady state (Study A), therefore we are quite confident about our results. The simulations of our PBPK model were then used for comparison with the established MRLs in Europe. In order not to exceed these thresholds, European regulatory authorities established [6], after a depletion study, a withdrawal time after cessation of treatment of 3 or 4 days for Marbocyl© before slaughter[9]. Our popPBPK model predictions also established that the kidney was the tissue linked to the highest withdrawal time. The predicted withdrawal period was in

526 total agreement with these values as it was equal to 3.33 days rounded to 4 days, thus giving another
527 good confidence in this model. However, no regulatory recommendations will be made since PBPK
528 modeling is not the regulatory approach adopted for this determination. Indeed, despite their
529 physiological plausibility linking all tissues together, PBPK models still lack of recommendations
530 (guidelines) towards complementary studies, requested level of uncertainty and harmonization of
531 documentation for regulatory acceptance and use, particularly in the field of food safety and chemical
532 risk assessment[67-68]. Furthermore, as outlined by the GSA with Cmax in kidney (Fig. S7 A), the total
533 body clearance is a major sensitive parameter that very likely influences the predicted WP. This PK
534 parameter varies greatly between published studies, with a 3 fold-range (from 0.065 to 0.196 L/h/kg
535 BW) [10-12, 14, 20]. This huge variability may be explained by some physiological covariates, as the
536 pregnancy status[10] or the age-related changes, e.g. the maturational changes of eliminating organs
537 (such as kidneys, liver or intestine) as highlighted with PK study of MAR with pigs of different ages[12].
538 Due to the flexibility of PBPK models, including these physiological changes into the PBPK is
539 possible providing there is enough data to support them. These model refinements should help
540 adequately predicting the WP in pigs, at different life stages. However, we must emphasize again
541 that the use of MAR is not allowed in all countries for farm animal (e.g. in the US), even as an extra-
542 label use, and thus these results do not support such uses.
543 In this PBPK model, the total body clearance was divided into several fractions corresponding to the
544 known routes of elimination of MAR. The major elimination pathway is the renal one, which accounts
545 for about half of the total body clearance [12]. The elimination by intestinal secretion ($FE_{GUTWALL}$) was
546 the second most important pathway with an estimated value of about 40% of the total clearance
547 (Table S1). This is close to the value (30%) stated by the owner of the Marbocyl© speciality[8], giving
548 good confidence in our PBPK model. The fraction of elimination by hepatic biotransformation
549 ($FE_{METABOLIC}$) was extracted from the study of Schneider et al.[12]. This value (6.5%) likely represents
550 the minimum value of MAR biotransformation extent as it is the percentage of MAR dose which has
551 been eliminated in urine as metabolites. Indeed, MAR could also be transformed into metabolites
552 that are not excreted in urine. However, as this represents a rather minor elimination route (<10% of
553 total clearance), its impact is likely negligible. Finally, the use of the data of Study B from Ferran et

554 al.[20], and especially the biliary concentrations data (see Fig. S2), allowed us to estimate the biliary
555 excretion of MAR (FE_{BILE}) at a very low fraction equal to 0.5% (Table S1). However, to simplify our
556 model the bile excretion flow (WK_{bile}) was assumed as a constant flow rate, which does not
557 correspond to the physiological conditions of bile secretion for pigs. Indeed, the bile excretion follows
558 a fluctuating rhythm and depends on the moment of food ingestion[73]. In the future and with more
559 observed data, it would be possible to refine the biliary sub-model and to take into account the bile
560 flow mimicking the physiological conditions as already modeled elsewhere [74].
561 The elimination of MAR towards intestines is important in pigs[20-21] and this was outlined by the PBPK
562 model. For this intestinal secretion, we assumed that the P-gp transporter is the only efflux
563 transporter of MAR, and based on its protein expression in the gut wall of pigs [31-33], a subdivision of
564 $FE_{GUTWALL}$ was implemented although there was some discrepancies in these literature data.
565 Furthermore, in addition to the P-gp, MAR could be a substrate of other transporters of the ATP-
566 Binding Cassette (ABC) superfamily, including, BCRP and MRP2, which is for instance the case of
567 danofloxacin [75], another fluoroquinolone.
568 Overall, the model adequately predicted the observed concentrations within all segments of the small
569 intestines (Fig. 3). This is illustrated by the good results of the statistical analyses (MAPE, 2 and 3
570 fold-interval) despite a R^2 being slightly below 0.75 (Fig. S5). One limitation concerns the chemical
571 uptake in the intestines that has not been modelled due to the lack of data after oral treatments. This
572 could affect the kinetics within the intestinal contents. Therefore, the estimated value of (absolute)
573 intestinal secretion ($FE_{GUTWALL}$) should be refined in the future.
574 However, the model was not able to predict the observed data within the large intestine, especially
575 within the distal colon. Yet, the estimated transit constants in colon (Kc1 and Kc2) allowed us to
576 properly describe the MAR concentrations in this compartment during the calibration, except for the
577 last time point of study B (see Fig. S4). These estimated values appear to be not physiologically
578 realistic (implicating a too fast transit in those segments), which is a limitation of this part of the PBPK
579 model. Moreover, like for the other intestinal parts, the distal colon was modeled with a continuous
580 transit although this segment corresponds to the defecation compartment. Its transit would be rather
581 discrete[76] with successive and non-continuous defecations, which are very variable from one pig to

another. Unfortunately, to our knowledge, such a defecation model does not exist in the literature for pigs. Another source of variability is the type of diet which can greatly varies between studies. Indeed, fibrous content of the meals has an impact on the transit times [36].

Fortunately, the low reliable predictions of MAR concentrations in the large intestine does not preclude the use of the PBPK model to predict the MAR kinetics in the contents of the small intestines and its impact on the commensal bacteria. Indeed, these regional concentrations are of great interest to explore the bacterial resistance issue, as it is a major reservoir of bacteria such as *Escherichia coli* that are impacted by the high MAR concentrations[20]. A previous pharmacodynamic (PD) model was developed by our laboratory based on *in vitro* experiments with MAR and *E. coli* strains mimicking the intestinal content conditions[77]. Connecting the PBPK model developed here with this kind of PD models would be a useful tool to predict the bacterial resistance selection and the adaptation of the PBPK model allows to explore different scenario (different doses, different routes of administration, different physiological states)[78]. The ultimate step would be to integrate the PBPK-PD model with an on-farm model of bacterial transmission in order to assess the risk of resistant bacteria spread among pigs and be able to quantify the impact of interventions such as different cleaning protocols or isolation measures[79], and consider the subsequent risk posed to later parts of the food chain.

In conclusion, this PBPK model developed for MAR has an overall good predictability ability for the concentrations in all edible tissues and allowed us to compare the predicted withdrawal period predicted to the European regulatory ones. The PBPK sub-model of secretion and transit in the intestinal lumen of pigs allowed a comparison with measured concentrations in these compartments. It will require advances from the scientific community and standardization on both, relevant physio-pharmacological data (volumes, transit, efflux pumps expression and their variability) or events occurring at discrete or periodic times (biliary secretion and defecation). In the future, the PBPK model could be used to predict the kinetic of MAR concentrations in ileum (or other region of interest) and explore the risk of bacterial resistance development.

Abbreviations

ABC, ATP-Binding Cassette; ATP, Adenosine triphosphate; AUC, Area Under The Time Concentration Curve; BCRP, Breast Cancer Resistance Protein; BLQ, Below The Limit Of Quantification; BW, Bodyweight; C_{max}, Maximal Concentration; CV, Coefficients Of Variation; DNA, Deoxyribonucleic acid; EMEA, European Medicines Agency, EU, European Union; FAST, Fourier Amplitude Sensitivity Test; GOF, Goodness Of Fit; GSA, Global Sensitivity Analyses; HPLC, High Performance Liquid Chromatography; ID, Identifier; IIV, Inter-Individual Variability; LOD, Limit Of Detection; LOQ, Limit Of Quantification; MAR, Marbofloxacin, MAPE: mean absolute percentage error, MLR, The maximum residue limit; MRP2, Multidrug Resistance-Associated Protein 2; OECD, Organization for Economic Co-operation and Development; PBPK, Physiologically Based Pharmacokinetics; PD, Pharmacodynamics; PI, Prediction Interval; popPBPK, Population Physiologically Based Pharmacokinetic Model; qIVIVE, Quantitative *In Vitro To In Vivo* Extrapolation; R^2, Coefficient Of Determination; RSE, Relative Standard Errors; RV, Residual Variability; SAEM, Stochastic Approximation Expectation–Maximization; TCA, Trichloracetic Acid; VPC, Visual Predictive check; WHO, World Health Organization;

Supporting Information

Supporting Information: Additional figures for the calibration and validation of the PBPK model, details on observed data used for calibration, performance of the analytical method, evaluation of the PBPK model and PBPK model code. This information is available free of charge at the ACS Paragon Plus website

Acknowledgements

The authors sincerely thank Aude Ferran and Delphine Bibbal (INTHERES, Toulouse, France) for providing their raw data (Study B).

Funding sources

This study was funded by the French agency for food, environmental and occupational health & safety (Anses).

REFERENCES

1. Toutain, P.-L.; Ferran, A. A.; Bousquet-Melou, A.; Pelligand, L.; Lees, P., Veterinary medicine needs new green antimicrobial drugs. *Frontiers in microbiology* **2016,** *7*, 1196.
2. Benet, L. Z.; Zia-Amirhosseini, P., Basic principles of pharmacokinetics. *Toxicol Pathol* **1995,** *23* (2), 115-123.
3. Clewell, H. J.; Andersen, M. E., Physiologically-based pharmacokinetic modeling and bioactivation of xenobiotics. *Toxicol Ind Health* **1994,** *10* (1-2), 1-24.
4. Khalil, F.; Läer, S., Physiologically based pharmacokinetic modeling: methodology, applications, and limitations with a focus on its role in pediatric drug development. *J Biomed Biotechnol* **2011,** *2011*, 907461.
5. Giguère, S.; Dowling, P. M., Fluoroquinolones. *Antimicrobial therapy in veterinary medicine* **2013**, 295-314.
6. EMA, EMEA/MRL/693/99-FINAL. Marbofloxacin Summary Report (2). **2000**.
7. Cerniglia, C. E.; Kotarski, S., Evaluation of Veterinary Drug Residues in Food for Their Potential to Affect Human Intestinal Microflora. *Regulatory Toxicology and Pharmacology* **1999,** *29* (3), 238-261.
8. Vetoquinol. *Marbofloxacin reference book.*; France, 1999.
9. EMA Public interface of the Union Product Database (UPD) of all veterinary medicines authorised in the EU/EEA. https://medicines.health.europa.eu/veterinary/en (accessed July 2022).
10. Petracca, K.; Riond, J. L.; Graser, T.; Wanner, M., Pharmacokinetics of the gyrase inhibitor marbofloxacin: influence of pregnancy and lactation in sows. *Zentralbl Veterinarmed A* **1993,** *40* (1), 73-79.
11. Ding, H.; Li, Y.; Chen, Z.; Rizwan-ul-Haq, M.; Zeng, Z., Plasma and tissue cage fluid pharmacokinetics of marbofloxacin after intravenous, intramuscular, and oral single-dose application in pigs. *J Vet Pharmacol Ther* **2010,** *33* (5), 507-510.
12. Schneider, M.; Paulin, A.; Dron, F.; Woehrlé, F., Pharmacokinetics of marbofloxacin in pigs after intravenous and intramuscular administration of a single dose of 8 mg/kg: dose proportionality, influence of the age of the animals and urinary elimination. *J Vet Pharmacol Ther* **2014,** *37* (6), 523-530.
13. Yang, F.; Liu, Y.; Li, Z.; Wang, Y.; Liu, B.; Zhao, Z.; Zhou, B.; Wang, G., Tissue distribution of marbofloxacin in pigs after a single intramuscular injection. *J Vet Sci* **2017,** *18* (2), 169-173.
14. Cox, S. K., Allometric scaling of marbofloxacin, moxifloxacin, danofloxacin and difloxacin pharmacokinetics: a retrospective analysis. *J Vet Pharmacol Ther* **2007,** *30* (5), 381-386.
15. Sörgel, F.; Naber, K. G.; Kinzig, M.; Mahr, G.; Muth, P., Comparative pharmacokinetics of ciprofloxacin and temafloxacin in humans: a review. *The American journal of medicine* **1991,** *91* (6), S51-S66.
16. Rubinstein, E.; St. Julien, L.; Ramon, J.; Dautrey, S.; Farinotti, R.; Huneau, J.-F.; Carbon, C., The intestinal elimination of ciprofloxacin in the rat. *Journal of Infectious Diseases* **1994,** *169* (1), 218-221.
17. Ramon, J.; Dautrey, S.; Farinoti, R.; Carbon, C.; Rubinstein, E., Intestinal elimination of ciprofloxacin in rabbits. *Antimicrobial agents and chemotherapy* **1994,** *38* (4), 757-760.
18. Wiuff, C.; Lykkesfeldt, J.; Aarestrup, F. M.; Svendsen, O., Distribution of enrofloxacin in intestinal tissue and contents of healthy pigs after oral and intramuscular administrations. *J Vet Pharmacol Ther* **2002,** *25* (5), 335-342.
19. Pellet, T. Etude pharmacocinétique/pharmacodynamique de l'antibiorésistance dans la flore fécale : impact d'un traitement à la marbofloxacine par voie parentérale continue et pulsée sur l'émergence d'Escherichia coli fécaux résistants aux fluoroquinolones chez le porcelet sevré. These de doctorat, Rennes 1, 2006.
20. Ferran, A. A.; Bibbal, D.; Pellet, T.; Laurentie, M.; Gicquel-Bruneau, M.; Sanders, P.; Schneider, M.; Toutain, P.-L.; Bousquet-Melou, A., Pharmacokinetic/pharmacodynamic assessment of the effects of parenteral administration of a fluoroquinolone on the intestinal microbiota: comparison of bactericidal activity at the gut versus the systemic level in a pig model. *Int J Antimicrob Agents* **2013,** *42* (5), 429-435.
21. Pellet, T. Etude pharmacocinétique/pharmacodynamique de l'antibiorésistance dans la flore fécale: impact d'un traitement à la marbofloxacine par voie parentérale continue et pulsée sur l'émergence d'Escherichia coli fécaux résistants aux fluoroquinolones chez le porcelet sevré. Doctoral dissertation, Rennes 1, France, 2006.

22. Oh, H.; Nord, C. E.; Barkholt, L.; Hedberg, M.; Edlund, C., Ecological disturbances in intestinal microflora caused by clinafloxacin, an extended-spectrum quinolone. *Infection* **2000,** *28* (5), 272-277.
23. Wells, D. M.; James, O. B., Transmission of infectious drug resistance from animals to man. *Epidemiology & Infection* **1973,** *71* (1), 209-215.
24. Founou, L. L.; Founou, R. C.; Essack, S. Y., Antibiotic Resistance in the Food Chain: A Developing Country-Perspective. *Frontiers in Microbiology* **2016,** *7*.
25. Nestorov, I. A.; Aarons, L. J.; Arundel, P. A.; Rowland, M., Lumping of Whole-Body Physiologically Based Pharmacokinetic Models. *J Pharmacokinet Pharmacodyn* **1998,** *26* (1), 21-46.
26. Leavens, T. L.; Borghoff, S. J., Physiologically based pharmacokinetic model of methyl tertiary butyl ether and tertiary butyl alcohol dosimetry in male rats based on binding to α2u-globulin. *Toxicological sciences* **2009,** *109* (2), 321-335.
27. Yang, F.; Yang, Y. R.; Wang, L.; Huang, X. H.; Qiao, G.; Zeng, Z. L., Estimating marbofloxacin withdrawal time in broiler chickens using a population physiologically based pharmacokinetics model. *J Vet Pharmacol Ther* **2014,** *37* (6), 579-588.
28. Lin, Z.; Li, M.; Wang, Y. S.; Tell, L. A.; Baynes, R. E.; Davis, J. L.; Vickroy, T. W.; Riviere, J. E., Physiological parameter values for physiologically based pharmacokinetic models in food-producing animals. Part I: Cattle and swine. *J Vet Pharmacol Ther* **2020,** *43* (5), 385-420.
29. Juste, C.; Corring, T.; Le Coz, Y., Bile restitution procedures for studying bile secretion in fistulated pigs. *Lab Anim Sci* **1983,** *33* (2), 199-202.
30. Alvarez, A. I.; Pérez, M.; Prieto, J. G.; Molina, A. J.; Real, R.; Merino, G., Fluoroquinolone Efflux Mediated by ABC Transporters. *Journal of Pharmaceutical Sciences* **2008,** *97* (9), 3483-3493.
31. Tang, H.; Pak, Y.; Mayersohn, M., Protein expression pattern of P-glycoprotein along the gastrointestinal tract of the yucatan micropig. *J. Biochem. Mol. Toxicol.* **2004,** *18* (1), 18-22.
32. Gao, X.; Bhattacharya, S.; Chan, W. K.; Jasti, B. R.; Upadrashta, B.; Li, X., Expression of P-glycoprotein and CYP3A4 along the porcine oral-gastrointestinal tract: implications on oral mucosal drug delivery. *Drug Dev Ind Pharm* **2014,** *40* (5), 599-603.
33. Guo, T.; Huang, J.; Zhang, H.; Dong, L.; Guo, D.; Guo, L.; He, F.; Bhutto, Z. A.; Wang, L., Abcb1 in Pigs: Molecular cloning, tissues distribution, functional analysis, and its effect on pharmacokinetics of enrofloxacin. *Sci Rep* **2016,** *6* (1), 32244.
34. Sambrook, I. E., Studies on the flow and composition of bile in growing pigs. *J Sci Food Agric* **1981,** *32* (8), 781-791.
35. Merchant, H. A.; McConnell, E. L.; Liu, F.; Ramaswamy, C.; Kulkarni, R. P.; Basit, A. W.; Murdan, S., Assessment of gastrointestinal pH, fluid and lymphoid tissue in the guinea pig, rabbit and pig, and implications for their use in drug development. *Eur J Pharm Sci* **2011,** *42* (1-2), 3-10.
36. Wilfart, A.; Montagne, L.; Simmins, H.; Noblet, J.; Milgen, J. v., Digesta transit in different segments of the gastrointestinal tract of pigs as affected by insoluble fibre supplied by wheat bran. *Br J Nutr* **2007,** *98* (1), 54-62.
37. Yang, F.; Liu, H.; Li, M.; Ding, H.; Huang, X.; Zeng, Z., Use of a Monte Carlo analysis within a physiologically based pharmacokinetic model to predict doxycycline residue withdrawal time in edible tissues in swine. *Food Additives & Contaminants: Part A* **2012,** *29* (1), 73-84.
38. Lautz, L. S.; Dorne, J. L. C. M.; Oldenkamp, R.; Hendriks, A. J.; Ragas, A. M. J., Generic physiologically based kinetic modelling for farm animals: Part I. Data collection of physiological parameters in swine, cattle and sheep. *Toxicol Lett* **2020,** *319*, 95-101.
39. Huang, L.; Lin, Z.; Zhou, X.; Zhu, M.; Gehring, R.; Riviere, J. E.; Yuan, Z., Estimation of residue depletion of cyadox and its marker residue in edible tissues of pigs using physiologically based pharmacokinetic modelling. *Food Addit Contam Part A Chem Anal Control Expo Risk Assess* **2015,** *32* (12), 2002-2017.
40. Vilalta, C.; Giboin, H.; Schneider, M.; El Garch, F.; Fraile, L., Pharmacokinetic/pharmacodynamic evaluation of marbofloxacin in the treatment of Haemophilus parasuis and Actinobacillus pleuropneumoniae infections in nursery and fattener pigs using Monte Carlo simulations. *J Vet Pharmacol Ther* **2014,** *37* (6), 542-549.

41. Ferrer, J.; Scott, W. E.; Weegman, B. P.; Suszynski, T. M.; Sutherland, D. E. R.; Hering, B. J.; Papas, K. K., Pig Pancreas Anatomy: Implications for Pancreas Procurement, Preservation, and Islet Isolation. *Transplantation* **2008,** *86* (11), 1503-1510.
42. Boysen, S. R.; Caulkett, N. A.; Brookfield, C. E.; Warren, A.; Pang, J. M., Splenectomy Versus Sham Splenectomy in a Swine Model of Controlled Hemorrhagic Shock. *Shock: Injury, Inflammation, and Sepsis: Laboratory and Clinical Approaches* **2016,** *46* (4), 439-446.
43. Henze, L. J.; Koehl, N. J.; Bennett-Lenane, H.; Holm, R.; Grimm, M.; Schneider, F.; Weitschies, W.; Koziolek, M.; Griffin, B. T., Characterization of gastrointestinal transit and luminal conditions in pigs using a telemetric motility capsule. *European Journal of Pharmaceutical Sciences* **2021,** *156*, 105627.
44. Kuhn, E.; Lavielle, M., Maximum likelihood estimation in nonlinear mixed effects models. *Computational Statistics & Data Analysis* **2005,** *49* (4), 1020-1038.
45. Beal, S. L., Ways to fit a PK model with some data below the quantification limit. *J Pharmacokinet Pharmacodyn* **2001,** *28* (5), 481-504.
46. Fenneteau, F.; Li, J.; Nekka, F., Assessing drug distribution in tissues expressing P-glycoprotein using physiologically based pharmacokinetic modeling: identification of important model parameters through global sensitivity analysis. *J Pharmacokinet Pharmacodyn* **2009,** *36* (6), 495.
47. Tardiveau, J.; LeRoux-Pullen, L.; Gehring, R.; Touchais, G.; Chotard-Soutif, M. P.; Mirfendereski, H.; Paraud, C.; Jacobs, M.; Magnier, R.; Laurentie, M.; Couet, W.; Marchand, S.; Viel, A.; Grégoire, N., A physiologically based pharmacokinetic (PBPK) model exploring the blood-milk barrier in lactating species - A case study with oxytetracycline administered to dairy cows and goats. *Food and Chemical Toxicology* **2022,** *161*, 112848.
48. Physiologically Based Pharmacokinetic (PBPK) Modeling. In *Physiologically Based Pharmacokinetic (PBPK) Modeling*, Fisher, J. W.; Gearhart, J. M.; Lin, Z., Eds. Academic Press: 2020; pp i-iii.
49. Inter-Organization Programme for the Sound Management of, C. *Characterization and application of physiologically based phamacokinetic models in risk assessment*; World Health Organization: 2010, 2010.
50. Guidance document on the characterisation, validation and reporting of physiologically based kinetic (PBK) models for regulatory purposes, OECD Series on Testing and Assessment, No. 331, Environment, Health and Safety, Environment Directorate, Organisation for Economic Co-operation and Development (OECD). 2021.
51. Lautz, L. S.; Hoeks, S.; Oldenkamp, R.; Hendriks, A. J.; Dorne, J. L. C. M.; Ragas, A. M. J., Generic physiologically based kinetic modelling for farm animals: Part II. Predicting tissue concentrations of chemicals in swine, cattle, and sheep. *Toxicol Lett* **2020,** *318*, 50-56.
52. Chou, W.-C.; Tell, L. A.; Baynes, R. E.; Davis, J. L.; Maunsell, F. P.; Riviere, J. E.; Lin, Z., An Interactive Generic Physiologically Based Pharmacokinetic (igPBPK) Modeling Platform to Predict Drug Withdrawal Intervals in Cattle and Swine: A Case Study on Flunixin, Florfenicol and Penicillin G. *Toxicol Sci* **2022**, kfac056.
53. Lin, Z.; Cheng, Y.-H.; Chou, W.-C.; Li, M., Physiologically based pharmacokinetic model calibration, evaluation, and performance assessment. In *Physiologically Based Pharmacokinetic (PBPK) Modeling*, Elsevier: 2020; pp 243-279.
54. Chevance, A.; Jacques, A. M.; Laurentie, M.; Sanders, P.; Henri, J., The present and future of withdrawal period calculations for milk in the European Union: focus on heterogeneous, nonmonotonic data. *J Vet Pharmacol Ther* **2017,** *40* (3), 218-230.
55. Saltelli, A.; Bolado, R., An alternative way to compute Fourier amplitude sensitivity test (FAST). *Computational Statistics & Data Analysis* **1998,** *26* (4), 445-460.
56. McNally, K.; Cotton, R.; Loizou, G. D., A workflow for global sensitivity analysis of PBPK models. *Frontiers in pharmacology* **2011,** *2*, 31.
57. Physiologically-Based Modeling. In *Physiologically-Based Pharmacokinetic (PBPK) Modeling and Simulations*, John Wiley & Sons, Inc.: Hoboken, NJ, USA, 2012; pp 13-16.
58. Jarrett, A. M.; Gao, Y.; Hussaini, M. Y.; Cogan, N. G.; Katz, D. F., Sensitivity Analysis of a Pharmacokinetic Model of Vaginal Anti-HIV Microbicide Drug Delivery. *Journal of Pharmaceutical Sciences* **2016,** *105* (5), 1772-1778.

59. Li, M.; Gehring, R.; Riviere, J. E.; Lin, Z., Development and application of a population physiologically based pharmacokinetic model for penicillin G in swine and cattle for food safety assessment. *Food and Chemical Toxicology* **2017,** *107*, 74-87.
60. Lixoft, S. A. S. *Monolix version 2021R1*, 2021; Antony, France, 2021.
61. Traynard, P.; Ayral, G.; Twarogowska, M.; Chauvin, J., Efficient Pharmacokinetic Modeling Workflow With the MonolixSuite: A Case Study of Remifentanil. *CPT: Pharmacometrics & Systems Pharmacology* **2020**.
62. Lixoft, S. A. S. *Simulix version 2021R1*, 2021; Antony, France, 2021.
63. *RStudio: Integrated Development Environment for R*, RStudio, PBC: Boston, MA, 2022.
64. Iooss B, V. S., Janon A, Pujol G, Broto wcfB, Boumhaout K, Delage T, Amri RE, Fruth J, Gilquin L, Guillaume J, Herin M, Idrissi MI, Le Gratiet L, Lemaitre P, Marrel A, Meynaoui A, Nelson BL, Monari F, Oomen R, Rakovec O, Ramos B, Roustant O, Song E, Staum J, Sueur R, Touati T, Verges V, Weber F. *sensitivity: Global Sensitivity Analysis of Model Outputs.* , R package version 1.27.0; 2021.
65. Lixoft, S. A. S. *lixoftConnectors: R connectors for Lixoft Suite* R package version 2021.1; 2019.
66. Corporation, M. *Microsoft Excel*, 2018.
67. Lautz, L. S.; Oldenkamp, R.; Dorne, J. L.; Ragas, A. M. J., Physiologically based kinetic models for farm animals: Critical review of published models and future perspectives for their use in chemical risk assessment. *Toxicology in Vitro* **2019,** *60*, 61-70.
68. Lin, Z.; Gehring, R.; Mochel, J.; Lave, T.; Riviere, J., Mathematical modeling and simulation in animal health–Part II: Principles, methods, applications, and value of physiologically based pharmacokinetic modeling in veterinary medicine and food safety assessment. *J Vet Pharmacol Ther* **2016,** *39* (5), 421-438.
69. Jones, H.; Rowland-Yeo, K., Basic concepts in physiologically based pharmacokinetic modeling in drug discovery and development. *CPT: pharmacometrics & systems pharmacology* **2013,** *2* (8), 1-12.
70. Chan, J. C.; Tan, S. P.; Upton, Z.; Chan, E. C., Bottom-up physiologically-based biokinetic modelling as an alternative to animal testing. *ALTEX-Alternatives to animal experimentation* **2019,** *36* (4), 597-612.
71. Sanquer, A.; Wackowiez, G.; Havrileck, B., Critical review on the withdrawal period calculation for injection site residues. *J Vet Pharmacol Ther* **2006,** *29* (5), 355-364.
72. Reeves, P., Residues of veterinary drugs at injection sites. *J Vet Pharmacol Ther* **2007,** *30* (1), 1-17.
73. Laplace, J.; Ouaissi, M.; Germain, C.; Roger, A. In *L'excretion biliaire chez le porc. Influence des repas et role eventuel de récepteurs oddiens dans le contrôle du debit choledocien*, Ann. Zootech., 1977; pp 595-613.
74. Okour, M.; Brundage, R. C., Modeling Enterohepatic Circulation. *Curr Pharmacol Rep* **2017,** *3* (5), 301-313.
75. Schrickx, J. A.; Fink-Gremmels, J., Danofloxacin-mesylate is a substrate for ATP-dependent efflux transporters: Fluoroquinolone disposition by efflux transporters. *British Journal of Pharmacology* **2007,** *150* (4), 463-469.
76. Auffray, P.; Martinet, J.; Rérat, A.; Marcilloux, J. C., QUELQUES ASPECTS DU TRANSIT GASTRO-INTESTINAL CHEZ LE PORC. *Ann. Biol. anim. Bioch. Biophys.* **1967,** *7* (3), 261-279.
77. Andraud, M.; Chauvin, C.; Sanders, P.; Laurentie, M., Pharmacodynamic modeling of in vitro activity of marbofloxacin against Escherichia coli strains. *Antimicrobial agents and chemotherapy* **2011,** *55* (2), 756-761.
78. Sadiq, M. W.; Nielsen, E. I.; Khachman, D.; Conil, J.-M.; Georges, B.; Houin, G.; Laffont, C. M.; Karlsson, M. O.; Friberg, L. E., A whole-body physiologically based pharmacokinetic (WB-PBPK) model of ciprofloxacin: a step towards predicting bacterial killing at sites of infection. *J Pharmacokinet Pharmacodyn* **2017,** *44* (2), 69-79.
79. McCarthy, C.; Viel, A.; Gavin, C.; Sanders, P.; Simons, R. R., Estimating the likelihood of ESBL-producing E. coli carriage in slaughter-aged pigs following bacterial introduction onto a farm: A multiscale risk assessment. *Microbial Risk Analysis* **2022,** *20*, 100185.

Graphic for table of contents

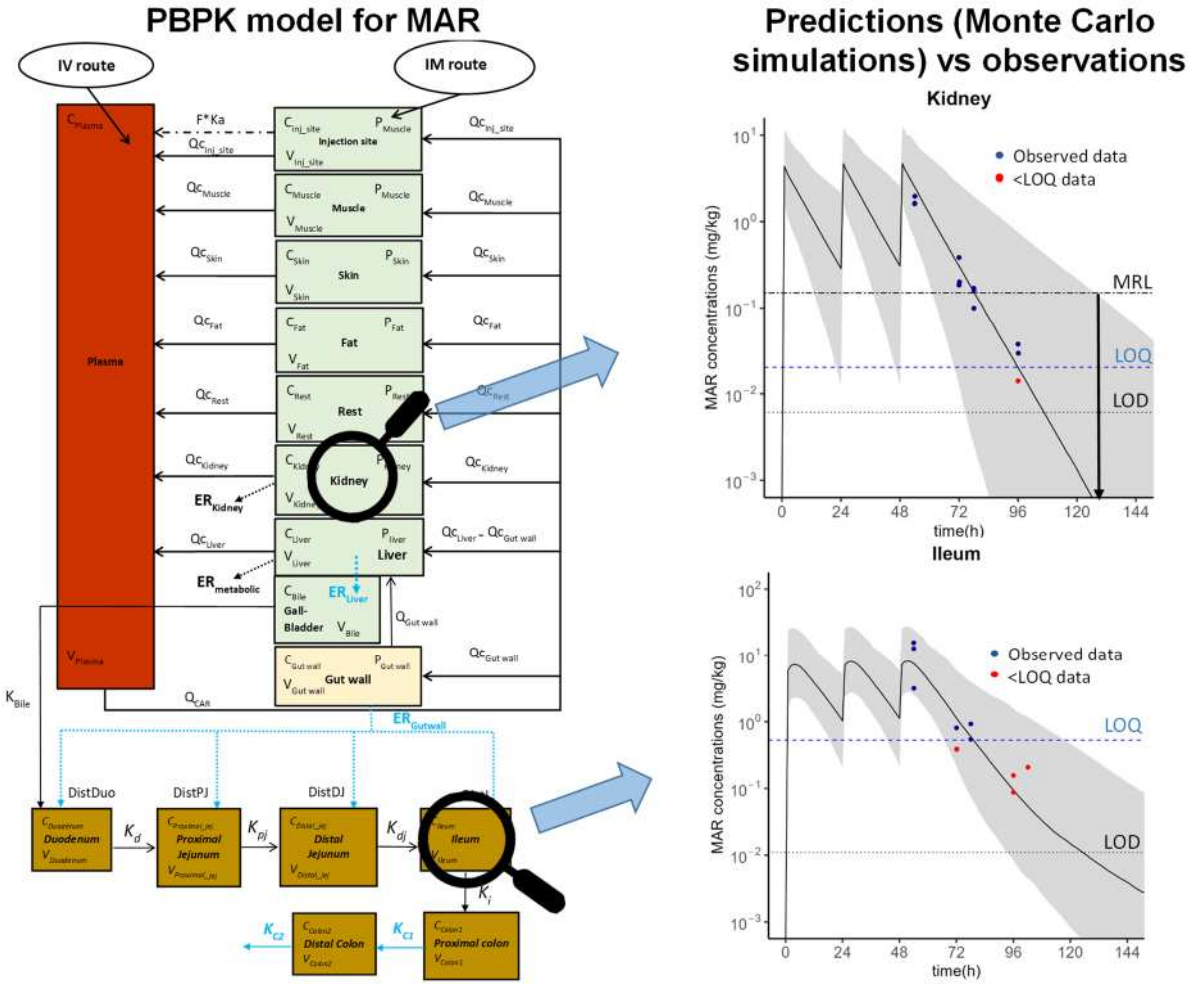

Supporting Information

A PBPK model to predict marbofloxacin distribution in edible tissues and intestinal exposure in pigs

Alexis Viel, Anis Nouichi, Mélanie Le Van Suu, Jean-Guy Rolland, Pascal Sanders, Michel Laurentie, Jacqueline Manceau, and Jerome Henri*

French Agency for Food, Environmental and Occupational Health & Safety (ANSES), Fougères Laboratory, 10B rue Claude Bourgelat, 35306 Fougères, France.

* Corresponding author at: French Agency for Food, Environmental and Occupational Health & Safety (ANSES), Fougères Laboratory, 10B rue Claude Bourgelat, 35306 Fougères, France.
Phone number: +33 (0)2 99 17 27 57 - E-mail address: jerome.henri@anses.fr

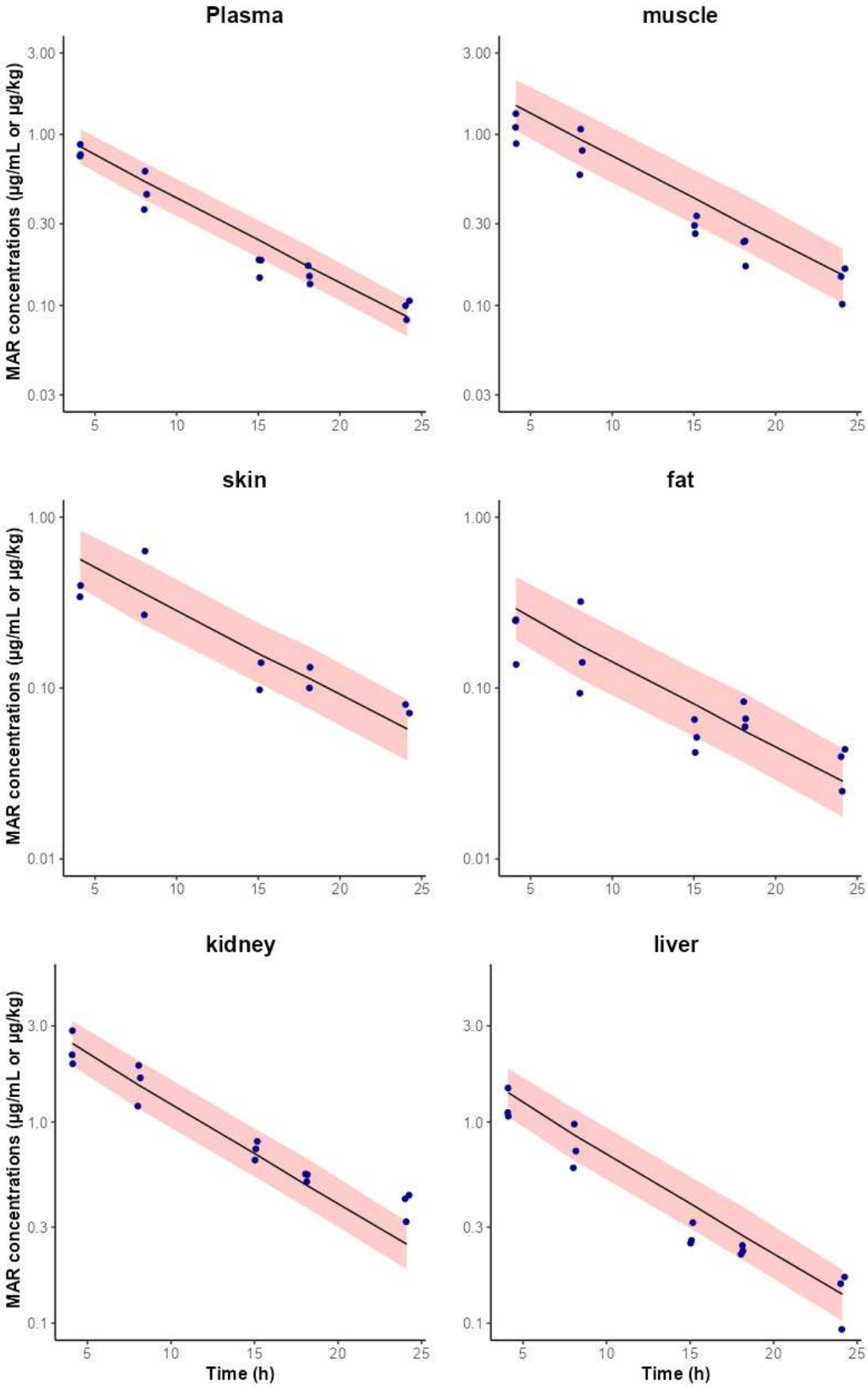

Figure S1. *Visual predictive check of concentrations in plasma and edible tissues of study A after calibration of the PBPK model. The median is represented by a dashed black line and the 90% prediction interval is represented by the red area. The experimental data (individual data points) are represented with circular blue points.*

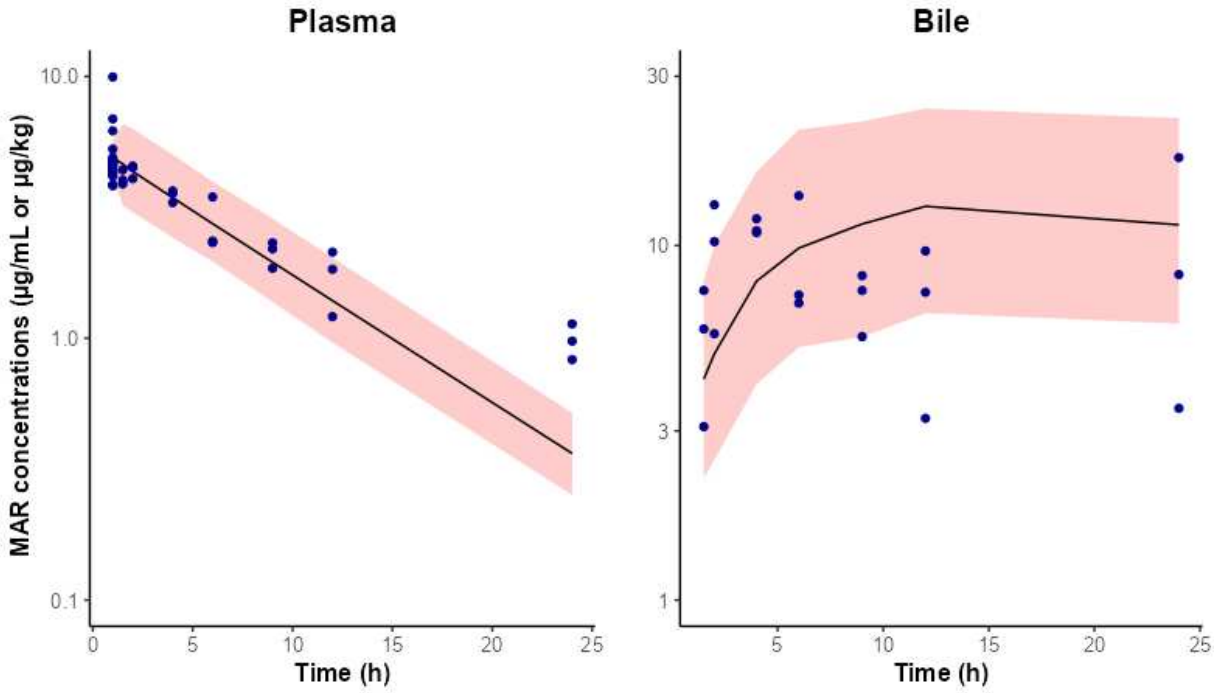

Figure S2. *Visual predictive check of concentrations in plasma and bile of study B after calibration of the PBPK model. The median is represented by a dashed black line and the 90% prediction interval is represented by the red area. The experimental data (individual data points) are represented with circular blue points.*

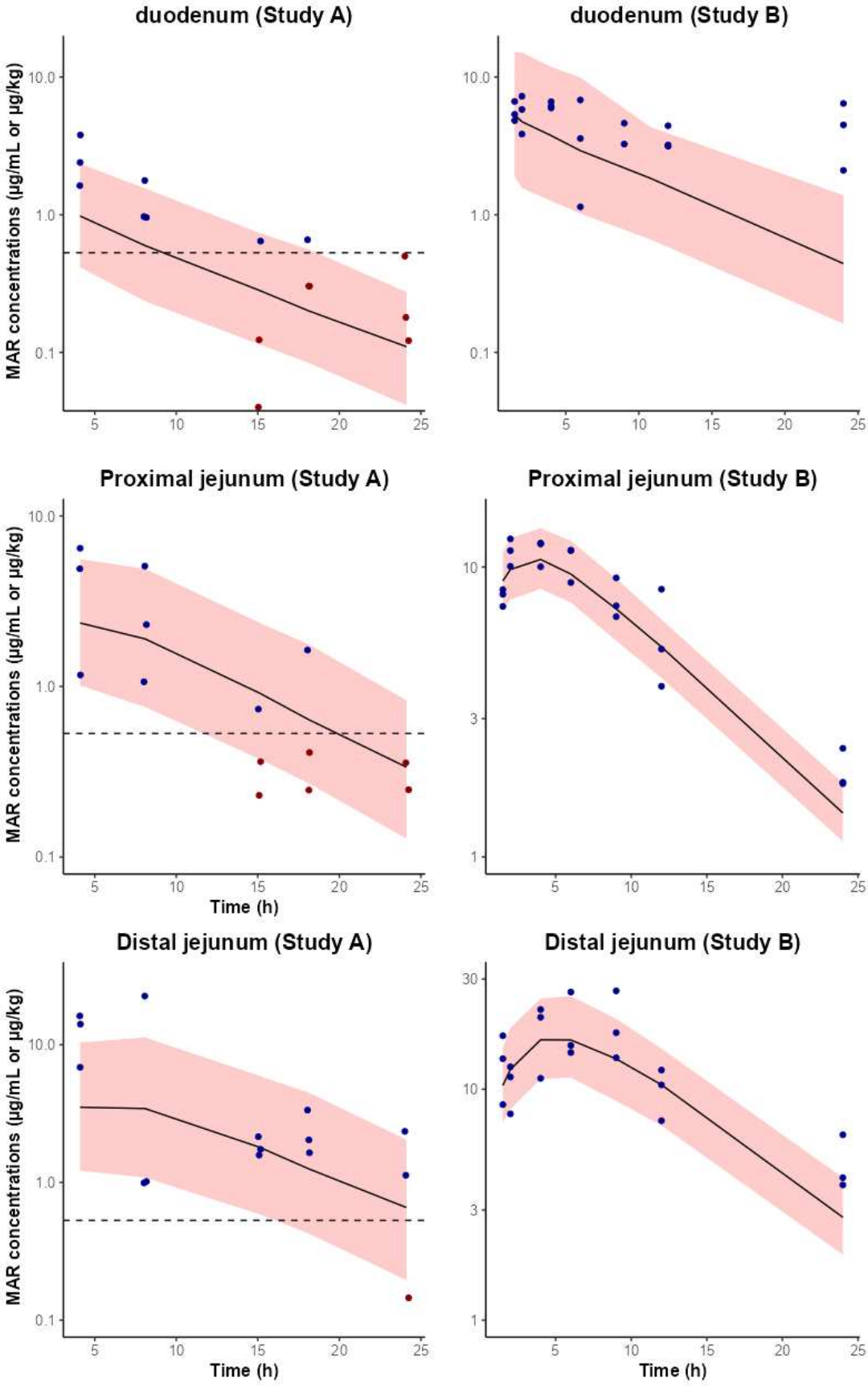

Figure S3. *Visual predictive check of concentrations in small intestines (Duodenum, Proximal jejunum and distal jejunum) after calibration of the PBPK model. The median is represented by a dashed black line and the 90% prediction interval is represented by the red area. The experimental data (individual data points) from each study are represented with circular blue points or with red points for the simulated data below the LOQ. Horizontal dashed line represents the LOQ.*

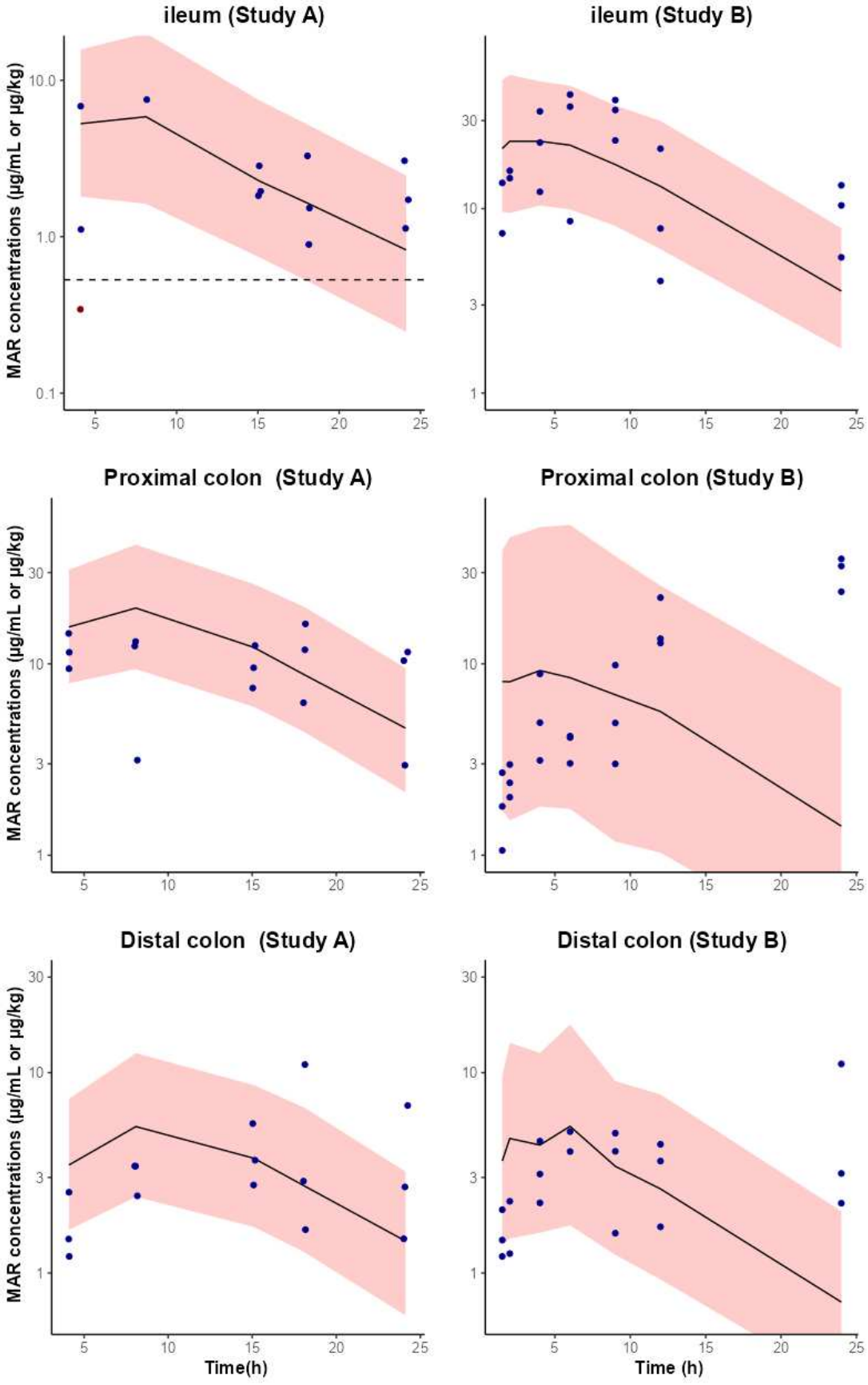

Figure S4. *Visual predictive check of concentrations in ileum and large intestines after calibration of the PBPK model. The median is represented by a dashed black line and the 90% prediction interval is represented by the red area. The experimental data (individual data points) from each study are represented with circular blue points or with red points for the simulated data below the LOQ. Horizontal dashed line represents the LOQ.*

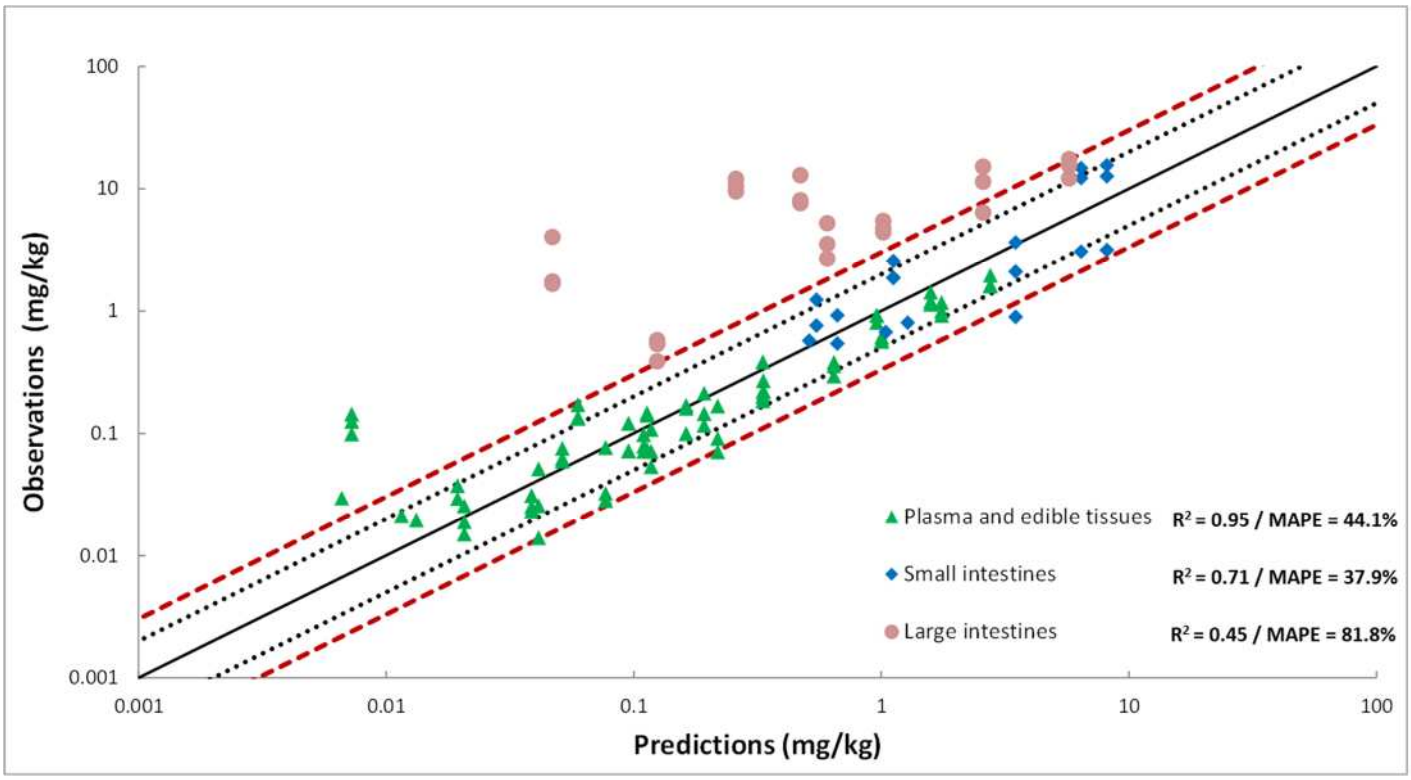

Figure S5. Regression analysis between model predictions and measured MAR concentrations in comestible tissues (plasma, skin, muscle, abdominal fat, liver & kidney), small intestine (duodenum, proximal and distal jejunum, ileum) and large intestine (proximal and distal colon). The solid black line represents the identity line, the dotted black lines represent the two-fold ratio and the dashed red lines represent the three-fold ratio. The coefficient of determination (R^2) and MAPE value are shown for different compartments of the PBPK model.

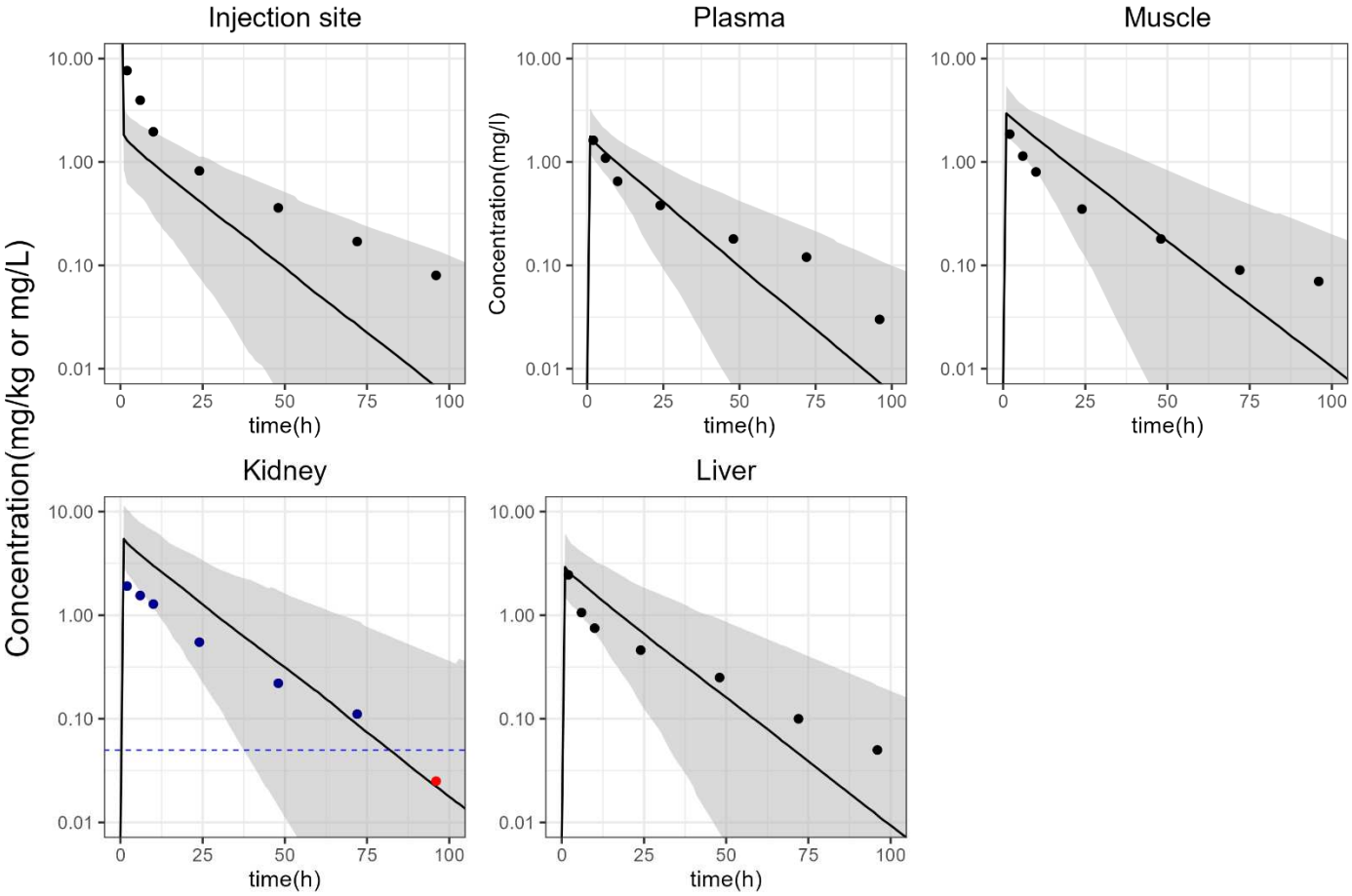

Figure S6. Distribution of predictions against external data from Yang *et al.,* 2017 in tissues and plasma after a single IM injection, with the total clearance value extracted from their data (0.08 L/h/kg). The solid black lines represents the median, and the grey areas represent 98% prediction intervals. The blue and red points represent the mean observations above and below the LOQ, respectively. Dashed blue line represents the LOQ. Of note, data below the LOQ were plotted at LOQ/2 for visualization purpose.

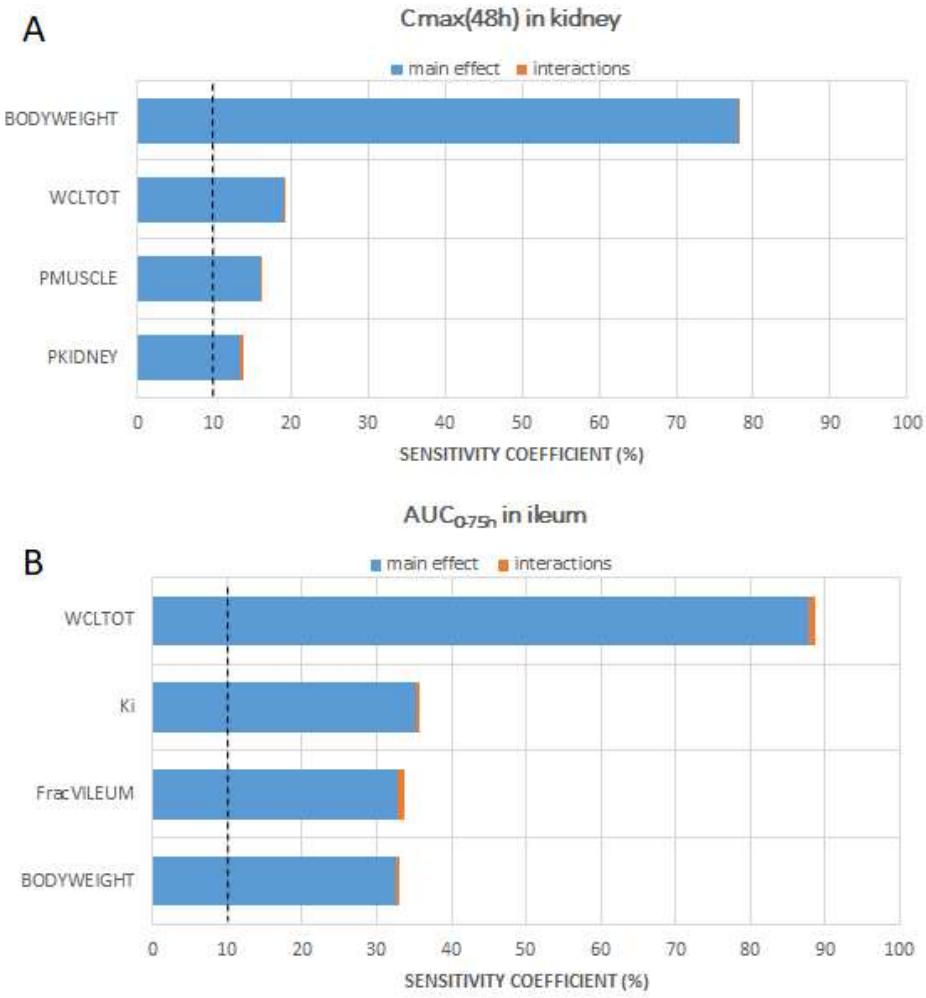

Figure S7. Global sensitivity analysis of the PBPK model. Sensitivity coefficient (%) were estimated for the $\mathbf{C_{max(49h)}}$ at the end of the treatment in kidney **(A)** and for $\mathbf{AUC_{0\text{-}75h}}$ in ileum **(B)**. The contribution of the main effect for each parameter is presented in blue while interactions contribution is presented in orange. The dotted lines represent the threshold of 10% for determining the impact of a parameter.

Table S1. *Results of the calibration of the PBPK model.*

	Parameters	Units	Estimation	RSE%
Fixed effect	Kc1 (study A)	h^{-1}	0.48	15.4
	Kc1 (study B)	h^{-1}	5.16	6.59
	Kc2 (study A)	h^{-1}	1.03	18.6
	Kc2 (study B)	h^{-1}	6.64	10.3
	$FE_{GUTWALL}$	%	41	0.009
	FE_{BILE}	%	0.49	4.79
Residual variability (CV)	plasma (Study B)	%	32	10.9
	plasma (Study A)	%	22	18.3
	muscle (Study A)	%	33	18.3
	skin (Study A)	%	35	22.4
	fat (Study A)	%	41	18.3
	kidney (Study A)	%	25	18.3
	liver (Study A)	%	26	18.3
	duodenum (Study B)	%	99	15.8
	duodenum (Study A)	%	83	26.5
	proximal jejunum (Study B)	%	22	15.4
	proximal jejunum (Study A)	%	82	21.6
	distal jejunum (Study B)	%	36	15.4
	distal jejunum (Study A)	%	103	18.7
	ileum (Study B)	%	70	16.2
	ileum (Study A)	%	104	14.7
	proximal colon (Study B)	%	150	15.4
	proximal colon (Study A)	%	66	18.3
	distal colon (Study B)	%	93	16.2
	distal colon (Study A)	%	73	18.3
	bile (Study B)	%	62	15.4

Table S2. *Performances of analytical methods for marbofloxacin quantification in the different pig matrices.*

Matrix (unit of concentration)	Mean introduced concentration	Recovery (%)	Repeatability (RSD%)	Intermediate precision (RSD%)	Relative bias (%)	LOQ (LOD) In unit of concentration
Plasma (µg/L)	25	105.9	1.649	1.649	-15.08	25.0 (0.3)
	50	99.61	0.3769	0.3769	-20.37	
	100	100.9	0.3297	0.8637	-19.48	
	500	97.55	1.047	1.047	-22.22	
	1000	96.53	0.2524	0.2524	-23.05	
	2500	98.72	0.2101	0.9563	-21.30	
Muscle (µg/kg)	15.1	90.40	3.508	3.508	-9.596	15.1 (4.6)
	50.32	96.80	1.095	2.454	-3.197	
	251.6	103.5	1.333	1.357	3.508	
	1006	103.1	0.8125	1.381	3.118	
	3019	102.5	1.760	1.890	2.526	
Kidney (µg/kg)	15.10	100.0	0.2854	4.555	0.03413	20.3 (6.1)
	50.32	99.59	1.785	1.785	-0.4075	
	251.6	102.3	0.6730	0.6730	2.302	
	1006	99.18	1.391	1.391	-0.8224	
	3019	98.94	0.9327	1.657	-1.061	
Liver (µg/kg)	15.1	98.23	0.3509	1.985	-1.771	15.1 (0.2)
	251.6	98.71	0.6885	2.985	-1.291	
	1006	94.58	1.012	1.012	-5.420	
	3019	96.82	0.6908	3.172	-3.176	
Fat (µg/kg)	15.1	97.16	2.269	3.194	-2.838	15.1 (0.2)
	50.32	98.97	1.767	4.122	-1.034	
	251.6	99.65	1.143	1.194	-0.3498	
	1006	102.5	2.041	5.247	2.458	
Skin (µg/kg)	15.1	97.46	2.624	2.624	-2.542	15.1 (4.6)
	50.32	99.21	0.7686	0.7686	-0.7876	
	251.6	102.6	1.322	1.322	2.552	
	1006	102.8	0.09937	0.6169	2.783	
	3019	98.00	2.930	4.659	-1.998	
Intestinal content (µg/kg)	531.1	94.70	1.232	2.175	3.072	531.1 (10.9)
	1062	101.7	1.519	2.304	-2.490	
	5311	101.6	4.202	4.444	-1.939	
	21245	102.3	3.949	4.898	0.9772	

Table S3. *Number of data below the LOQ for study A*

Tissue of study A	**Number of observed data <LOQ**
Plasma	0
Muscle	0
Liver	0
Kidney	0
Fat	0
Skin	0
Duodenum	7
Proximal jejunum	7
Distal jejunum	1
Ileum	1
Proximal Colon	0
Distal Colon	0
% of all observed data	**8.9**

Table S4. *Evaluation of the PBPK model.*

Categories	Characteristics
Scope and purpose of the model	- Model purpose: PBPK model of marbofloxacin including digestive tract - Species: Pig - Age, life stage(s), sex, exposure window(s): Piglets, males and females, single and multiple doses - Exposure route(s), and dose metric(s): IV and IM - Target organs and tissues: edible tissues and intestinal contents
Model structure and mathematical description	- Graphical representation of the model available - 16 compartments - Steady-state and differential calculations - Mass balance equations given
Computer implementation	- Model implemented in Monolix (Mlxtran language) - Model code is provided as supplementary materials Table S5.
Parameters estimation and analysis	- Anatomical and physiological parameter values from the literature, experimentally determined or predicted - Physicochemical and biochemical parameter values from literature or predicted
Model calibration and validation	- Global sensitivity analysis performed - Model calibrated with measured data from 2 different datasets - Calibration data and model calibration step adequately reported - Model validation against independent data (internal and external data) - Validation data reported - Variability analysis of the model predictions: predicted versus experimental data expressed as fold changes, MAPE
Model documentation	- Peer-reviewed model - Publicly available model

Table S5. *Model code in mlxtran*

```
[LONGITUDINAL]

input={PREST,Kc1,Kc2,BODYWEIGHT,WCLTOT,FEGUTWALL,FEKIDNEY,FEBILE,FEMETABOLIC,WKBILE,HAEMATOCRIT,FracVINJSIT
E,FracVMUSCLE,FracVFAT,FracVSKIN,FracVLIVER,FracVKIDNEY,FracVGUTWALL,FracVBLOOD,FracVDUODENUM,FracVJEJUNUM
1,FracVJEJUNUM2,FracVILEUM,FracVCOLON1,FracVCOLON2,FracVBILE,QTOT,FracQcInjsite,FracQcMuscle,FracQcFat,FracQcSki
n,FracQcKidney,FracQcLiver,FracQcGutWall,Kd,Kjp,Kjd,Ki,PMUSCLE,PFAT,PSKIN,PLIVER,PKIDNEY,PGUTWALL,F,ka,DistDuo,DistP
J,DistDJ,DistI}
BODYWEIGHT={use=regressor}

PK:
;----------------------------------------------------------------------------------------------------------
;;;;Creation of the different compartments;;;;
;----------------------------------------------------------------------------------------------------------

compartment(cmt=1,amount=Ap)      ;plasma compartment

compartment(cmt=2,amount=Am)      ;muscle compartment

compartment(cmt=3,amount=Af)       ;Fat compartment

compartment(cmt=4,amount=Ak)   ;Kidney compartment

compartment(cmt=5,amount=Al)   ;Liver compartment

compartment(cmt=6,amount=Ad)   ;duodenum compartment

compartment(cmt=7,amount=Ajp)  ; proximal jejunum compartment

compartment(cmt=8,amount=Ai)   ;ileum compartment

compartment(cmt=9,amount=Ac1)  ; proximal colon  compartment

compartment(cmt=10,amount=As)   ;skin compartment

compartment(cmt=11,amount=Ajd)   ; distal jejunum compartment

compartment(cmt=12,amount=Ac2)  ; distal colon compartment

compartment(cmt=13,amount=Ar)    ;Rest compartment

compartment(cmt=14,amount=Agw)  ;Gut wall compartment

compartment(cmt=15,amount=Ais)   ;injection site compartment;

compartment(cmt=16,amount=Ab)   ;Bile compartment

;----------------------------------------------------------------------------------------------------------
```

```
;;;; Drug administration ;;;;
;-----------------------------------------------------------------------------------------------------------
iv(adm=1,cmt=1)    ;IV Bolus (Study A)

iv(adm=2,cmt=1)    ;infusion during 4 hours; (Study A)

depot(type=3, target=Ais, p=F)  ; depot compartment used for IM administration, linked to injection site (Study B)

EQUATION:
;;definition of the initial time;;
t_0=0

;-----------------------------------------------------------------------------------------------------------
;;;Physiological parameters;;;
;-----------------------------------------------------------------------------------------------------------

;Volumes of each compartment, as fraction of total body volume (see Table 2);
;FracVINJSITE=0.003   ;injection site compartment;
;FracVMUSCLE=0.45       ;muscle compartment
;FracVFAT=0.176     ;fat compartment
;FracVSKIN=0.0528     ;skin compartment
;FracVLIVER=0.017     ;liver compartment
;FracVKIDNEY=0.003     ;kidney compartment
;FracVGUTWALL=0.0519     ;gut wall compartment
;FracVBLOOD=0.0412     ;blood compartment
;FracVDUODENUM=0.0018      ;duodenum compartment
;FracVJEJUNUM1=0.018        ;distal jejunum compartment
;FracVJEJUNUM2=0.018       ;proximal jejunum compartment
;FracVILEUM=0.0018      ;ileum compartment
;FracVCOLON1=0.0046       ;proximal colon compartment
;FracVCOLON2=0.0077 ;      distal colon compartment
;FracVBILE=0.00175             ; (2100ml/24h/50kg)

;-----------------------------------------------------------------------------------------------------------
;Adjusted Volumes for simulation, avoid unrealistic negative values during simulation of the popPBPK model
FracVVREST=1-
(FracVMUSCLE+FracVFAT+FracVSKIN+FracVLIVER+FracVKIDNEY+FracVBLOOD+FracVDUODENUM+FracVJEJUNUM1+FracVJEJU
NUM2+FracVILEUM+FracVCOLON1+FracVCOLON2+FracVBILE)

if FracVVREST <0
FracVREST=0
else
FracVREST=1-
(FracVMUSCLE+FracVFAT+FracVSKIN+FracVLIVER+FracVKIDNEY+FracVBLOOD+FracVDUODENUM+FracVJEJUNUM1+FracVJEJU
NUM2+FracVILEUM+FracVCOLON1+FracVCOLON2+FracVBILE)
end
FVadjust=FracVMUSCLE+FracVFAT+FracVSKIN+FracVLIVER+FracVKIDNEY+FracVBLOOD+FracVDUODENUM+FracVJEJUNUM1+Fr
acVJEJUNUM2+FracVILEUM+FracVCOLON1+FracVCOLON2+FracVBILE+FracVREST

;HAEMATOCRIT=0.412
```

```
;----------------------------------------------------------------------------------------------------------
; Blood flow of each compartment, as fraction of cardiac output (see Table 2);

;QTOT=8.7  ;l/h/kg, cardiac output
;FracQcInjsite=0.009
;FracQcMuscle=0.292
;FracQcFat=0.11
;FracQcSkin=0.035
;FracQcKidney=0.098
;FracQcLiver=0.225      ;(Hepatic Artery + Portal vein)
;FracQcGutWall=0.18     ;(Portal vein solely)
FracQQcRest=1-(FracQcInjsite+FracQcMuscle+FracQcFat+FracQcSkin+FracQcKidney+FracQcLiver)

;----------------------------------------------------------------------------------------------------------
;Adjusted Flows for simulation, avoid unrealistic negative values during simulation of the popPBPK model

if FracQQcRest <0
FracQcRest=0
else
FracQcRest=1-(FracQcInjsite+FracQcMuscle+FracQcFat+FracQcSkin+FracQcKidney+FracQcLiver)
end
FQadjust=FracQcInjsite+FracQcMuscle+FracQcFat+FracQcSkin+FracQcKidney+FracQcLiver+FracQcRest

;----------------------------------------------------------------------------------------------------------
;Digestive transit time, calculated according to the length of the different segments and based on Wilfart, 2007 (See Table 2)

;Kd=5.26     ;Duodenum transit constant
;Kjp=0.51    ;Proximal jejunum transit constant
;Kjd=0.51    ;Distal jejunum transit constant
;Ki=5.26     ;Ileum transit constant
;Kc1=0.06    ;initial value of Proximal colon transit constant
;Kc2=0.04    ;initial value of Distal colon transit constant

;----------------------------------------------------------------------------------------------------------
;Partition coefficients;

;PMUSCLE=1.66
;PFAT=0.33
;PSKIN=0.63
;PLIVER=1.73
;PKIDNEY=3.44
;PGUTWALL=0.83
; PREST = 1.86      ; calculated

;----------------------------------------------------------------------------------------------------------
Absolute compartment volume values
;----------------------------------------------------------------------------------------------------------

VINJSITE=(FracVINJSITE/FVadjust)*BODYWEIGHT
VMUSCLE=(FracVMUSCLE/FVadjust)*BODYWEIGHT
VFAT=(FracVFAT/FVadjust)*BODYWEIGHT
```

```
VSKIN=(FracVSKIN/FVadjust)*BODYWEIGHT
VLIVER=(FracVLIVER/FVadjust)*BODYWEIGHT
VKIDNEY=(FracVKIDNEY/FVadjust)*BODYWEIGHT
VREST=(FracVREST/FVadjust)*BODYWEIGHT
VPLASMA=(FracVBLOOD/FVadjust*BODYWEIGHT)*(1-HAEMATOCRIT)
VGUTWALL=(FracVGUTWALL/FVadjust)*BODYWEIGHT
VDUODENUM=(FracVDUODENUM/FVadjust)*BODYWEIGHT
VJEJUNUM1=(FracVJEJUNUM1/FVadjust)*BODYWEIGHT
VJEJUNUM2=(FracVJEJUNUM2/FVadjust)*BODYWEIGHT
VILEUM=(FracVILEUM/FVadjust)*BODYWEIGHT
VCOLON1=(FracVCOLON1/FVadjust)*BODYWEIGHT
VCOLON2=(FracVCOLON2/FVadjust)*BODYWEIGHT
VBILE=(FracVBILE/FVadjust)*BODYWEIGHT

;-----------------------------------------------------------------------------------------------------------
Absolute compartment blood flow values
;-----------------------------------------------------------------------------------------------------------

QcINJSITE=(FracQcInjsite/FQadjust)*QTOT
QcMUSCLE=(FracQcMuscle/FQadjust)*QTOT
QcFAT=(FracQcFat/FQadjust)*QTOT
QcSKIN=(FracQcSkin/FQadjust)*QTOT
QcKIDNEY=(FracQcKidney/FQadjust)*QTOT
QcLIVER=(FracQcLiver/FQadjust)*QTOT
QcGUTWALL=(FracQcGutWall/FQadjust)*QTOT
QcREST=(FracQcRest/FQadjust)*QTOT

;-----------------------------------------------------------------------------------------------------------
;;Definition of MAR concentrations in each compartment
;-----------------------------------------------------------------------------------------------------------

CINJSITE=Ais/VINJSITE
CtbINJSITE=CINJSITE/PMUSCLE   ; MAR concentration leaving the inj. site compartment

CMUSCLE=Am/VMUSCLE
CtbMUSCLE=CMUSCLE/PMUSCLE   ; MAR concentration leaving the muscle compartment

CFAT=Af/VFAT
CtbFAT=CFAT/PFAT   ; MAR concentration leaving the fat compartment

CSKIN=As/VSKIN
CtbSKIN=CSKIN/PSKIN   ; MAR concentration leaving the skin compartment

CLIVER=Al/VLIVER
CtbLIVER=CLIVER/PLIVER   ; MAR concentration leaving the liver compartment

CKIDNEY=Ak/VKIDNEY
CtbKIDNEY=CKIDNEY/PKIDNEY   ; MAR concentration leaving the kidney compartment
```

```
CREST=Ar/VREST
CtbREST=CREST/PREST   ; MAR concentration leaving the rest compartment

CGUTWALL=Agw/VGUTWALL
CtbGUTWALL=CGUTWALL/PGUTWALL   ; MAR concentration leaving the gutwall compartment

CPLASMA=Ap/VPLASMA   ; plasma MAR concentration

CBILE=Ab/VBILE     ; biliary MAR concentration

CDUODENUM=Ad/VDUODENUM     ; duodenal MAR concentration

CJEJUNUM1=Ajp/VJEJUNUM1     ;  proximal jejunum MAR concentration

CJEJUNUM2=Ajd/VJEJUNUM2     ; distal jejunum MAR concentration

CILEUM=Ai/VILEUM      ; ileum MAR concentration

CCOLON1=Ac1/VCOLON1      ; proximal colon MAR concentration

CCOLON2=Ac2/VCOLON2      ; distal colon MAR concentration
;-----------------------------------------------------------------------------------------------------------
;;Total clearance and fraction linked to different route of elimination (see Table 2)
;-----------------------------------------------------------------------------------------------------------
CLTOT=WCLTOT*BODYWEIGHT    ; total body clearance of MAR
FEadjust=FEKIDNEY+FEGUTWALL+FEBILE+FEMETABOLIC ; Sum of all clearance fraction
FracEKIDNEY=(FEKIDNEY/FEadjust)      ; Fraction of clearance linked to renal excretion
FracEBile=(FEBILE/FEadjust)      ; Fraction of clearance linked to biliary excretion
FracEGUTWALL=(FEGUTWALL/FEadjust)    ; Fraction of clearance linked to intestinal excretion
FracEMETABOLIC=(FEMETABOLIC/FEadjust)     ; Fraction of clearance linked to metabolism

;-----------------------------------------------------------------------------------------------------------
;;Sub-division of FracEGUTWALL in the different digestive sub-compartments;;
;DistDuo= 0.15    ; fraction linked to the duodenum
;DistPJ= 0.25    ; fraction linked to the proximal jejunum
;DistDJ= 0.30    ; fraction linked to the distal jejunum
;DistI= 0.30    ; fraction linked to the ileum
Distadjust=DistDuo+DistPJ+DistDJ+DistI

;; Bile flow from the gallbladder to the duodenum in l/h ;;
KBILE=WKBILE*BODYWEIGHT

;-----------------------------------------------------------------------------------------------------------
; DIFFERENTIAL EQUATIONS
;-----------------------------------------------------------------------------------------------------------
;Injection site compartment, receiving the IM injection;
ddt_Ais=(QcINJSITE*(CPLASMA-CtbINJSITE))-(ka*F*Ais)

;Muscle compartment;
```

```
ddt_Am=QcMUSCLE*(CPLASMA-CtbMUSCLE)

;Fat compartment;
ddt_Af=QcFAT*(CPLASMA-CtbFAT)

;Skin compartment;
ddt_As=QcSKIN*(CPLASMA-CtbSKIN)

;Liver compartment;
ddt_Al=((QcLIVER-QcGUTWALL)*CPLASMA)+(QcGUTWALL*CtbGUTWALL)-(CtbLIVER*QcLIVER)-(FracEBile * CLTOT*CPLASMA)-
(FracEMETABOLIC*CLTOT*CPLASMA)

;Kidney compartment;
ddt_Ak=QcKIDNEY*(CPLASMA-CtbKIDNEY)- (FracEKIDNEY * CLTOT  * CPLASMA)

;Plasma compartment;
ddt_Ap=ka*F*Ais+(QcINJSITE*CtbINJSITE)+(QcMUSCLE*CtbMUSCLE)+(QcFAT*CtbFAT)+(QcSKIN*CtbSKIN)+(QcREST*CtbREST)+
(QcKIDNEY*CtbKIDNEY)+(QcLIVER*CtbLIVER)-(QTOT*CPLASMA)

;duodenum compartment;
ddt_Ad=(KBILE*Ab)-(Kd*Ad)+((FracEGUTWALL*CLTOT*CPLASMA)*(DistDuo/Distadjust))

;jejunum proximal compartment;
ddt_Ajp=(Kd*Ad)-(Kjp*Ajp)+((FracEGUTWALL*CLTOT*CPLASMA)*(DistPJ/Distadjust))

;jejunum distal compartment;
ddt_Ajd=(Kjp*Ajp)-(Kjd*Ajd)+((FracEGUTWALL*CLTOT*CPLASMA)*(DistDJ/Distadjust))

;ileum compartment;
ddt_Ai=(Kjd*Ajd)-(Ki*Ai)+((FracEGUTWALL*CLTOT*CPLASMA)*(DistI/Distadjust))

; proximal colon compartment;
ddt_Ac1=(Ki*Ai)-(Kc1*Ac1)

;distal colon compartment;
ddt_Ac2=(Kc1*Ac1)-(Kc2*Ac2)

;Rest compartment;
ddt_Ar=QcREST*(CPLASMA-CtbREST)

;Gut Wall compartment;
ddt_Agw=QcGUTWALL*(CPLASMA-CtbGUTWALL)-(FracEGUTWALL*CLTOT*CPLASMA)

;Bile compartment;
ddt_Ab=(FracEBile * CLTOT*CPLASMA)-(KBILE*Ab)

OUTPUT:
output={CPLASMA,CMUSCLE,CSKIN,CFAT,CKIDNEY,CLIVER,CDUODENUM,CJEJUNUM1,CJEJUNUM2,
,CILEUM,CCOLON1,CCOLON2,CBILE}
```